

Operators' cognitive performance under extreme hot-humid exposure and its physiological-psychological mechanism based on ECG, fNIRS, and Eye Tracking

Yan Zhang^b, Ming Jia^a, Meng Li^b, JianYu Wang^b, XiangMin Hu^b, ZhiHui Xu^{a,*} and Tao Chen^{b,c,d,*}

^aState Key Laboratory of Nuclear Power Safety Technology and Equipment, China Nuclear Power Engineering Co., Ltd., Shenzhen, Guangdong, 518172, China

^bSchool of Safety Science, Tsinghua University, Beijing 100084, P.R. China

^cAnhui Province Key Laboratory of Human Safety, Hefei Anhui 230601, China

^dBeijing Key Laboratory of Comprehensive Emergency Response Science, Beijing, China

Abstract

Operators' cognitive and executive functions are impaired significantly under extreme heat stress, potentially resulting in more severe secondary disasters. This research investigated the impact of elevated temperature and humidity (25°C 60%RH, 30°C 70%RH, 35°C 80%RH, 40°C 90%RH) on the cognitive functions and performance of operators. Meanwhile, we explored the psychological-physiological mechanism underlying the change in performance by electrocardiogram (ECG), functional near-infrared spectroscopy (fNIRS), and eye tracking physiologically. Psychological aspects such as situation awareness, workload, and working memory were assessed. Eventually, we verified and extended the maximal adaptability model to the extreme condition. Unexpectedly, a temporary improvement in simple reaction tasks but rapid impairment in advanced cognitive functions (i.e. situation awareness, communication, working memory) was obtained above 35°C WBGT. The best performance in a suitable environment was due to more effective activation in the prefrontal cortex (PFC). With temperature increasing, more mistakes occurred and comprehension was impaired due to drowsiness and lower arousal levels, according to evidence of compensatory effect in fNIRS. In the extreme environment, the enhanced PFC cooperation with higher functional connectivity resulted in a temporary improvement, while depressed

*Corresponding author.

E-mail addresses: xuzhihui@hrbeu.edu.cn (Z.H. Xu), chentao.a@tsinghua.edu.cn (T. Chen).

activation in PFC, heavy physical load, and poor regulation of the cardiovascular system restricted it. Our results provide a more detailed study of the process of operators' performance and cognitive functions when encountering increasing heat stress, as well as its underlying mechanisms from a neuroergonomics perspective. This can contribute to a better understanding of the interaction between operators' performance and workplace conditions, and help to achieve a more reliable human-centered production system in the promising era of Industry 5.0.

Keywords: nuclear power plants; heat stress; cognitive performance; neuroergonomics; situation awareness; heart rate variability; functional connectivity; visual search pattern

1 INTRODUCTION

Industry 5.0 is pioneering a new engineering approach, focusing on human-centric solutions and emphasizing the importance of human beings in the systems (Xu et al., 2021). The cognitive and executive functions of operators are significantly impaired under intense and prolonged hot-humid exposure, potentially leading to more severe secondary disasters (thr, 2004). Within this context, it is vital to have a comprehensive understanding of the cognitive and reliability process of operators, both psychologically and physiologically, under intense heat stress in extremely hot and humid environments.

When individuals are exposed to an environment outside the range of thermal comfort, several typical cognitive and executive functions are significantly affected (Chen et al., 2020). The vigilant attention, automatic responses, and verbal memory are greatly impaired at 37.8°C compared to 21.°C, reflected by decreased performance in the serial reaction time test and the accuracy of the Stroop task (Yeoman et al., 2022). Improved cognitive abilities (including semantic interference and visual perception ability, spatial orientation ability, mental arithmetic ability, perception, attention, concentration, learning speed, short-term and long-term working memory, and arousal level) were observed at lower humidity (50% RH compared with 70% RH) (Tian et al., 2021). Furthermore, the participants' thinking, inattention, fatigue, and emotional levels showed significant improvements under lower humidity, as indicated by the subjective scales (Tian et al., 2021). The accuracy of cognitive functions (i.e., semantic interference, visual perception, spatial positioning, thinking, and arousal level) decreases notably at 37°C after a 45-minute moderate-intensity exercise, while the speed increased (Chen et al., 2020). As for risk tolerance, an important element in emergency handling, is affected at 50°C and 20% relative humidity, with less risk perception on the same risky behaviors and more risk-taking behaviors (Chang et al., 2017). For complex tasks such as perceptual-motor tasks including alertness, operating vehicle equipment, tracking, etc., the operational performance began to decrease significantly in the range of 30°C-33°C wet bulb globe temperature (WBGT)

(Ramsey, 1995).

Several hypotheses and models have been developed to gain a comprehensive understanding of the relationship between heat stress and operators' cognitive performance (Hancock and Vasmatazidis, 2003). The Yerkes-Dodson law, which explains the inverse U-shaped relationship between human performance and arousal level, has been migrated to explain the relationship between human performance and the thermal load, as heat stress is a critical factor in arousal level (Provins, 1966). On this basis, the maximal adaptability model (Hancock, 1989) has been proposed to improve validity and robustness. It reveals that a too-cold environment will lead to a lower arousal level and worse performance. When the temperature rises, individuals become more alert and perform better. When the temperature is within a certain suitable range, there is no obvious thermal impact on cognitive performance. This is because psychological and physiological states are within the adaptable range allowing cognitive resources to be dynamically adjusted to resist the influence of the thermal environment without compromising the main task performance. When the temperature keeps increasing, attention resources will be exhausted. Consequently, the human body is unable to allocate cognitive resources to primary tasks through self-regulation, resulting in a decline in performance. This hypothesis has been confirmed by several experiments. An inverted U-shaped relationship was fitted between the comprehensive heat stress index (reflecting the combination influence of physiological and subjective responses) and the accuracy of cognitive tests, while the speed of cognitive tests showed the opposite trends ($R^2 > 0.8$) (Liu et al., 2022). Heart rate, a potential biomarker of heat stress, has an inverted U-shaped relationship with the relative accuracy of various cognitive tests (Chen et al., 2023). A 4th order-function paradigm was fitted between the mean skin temperature and the relative cognitive performance (RCP), with a stable RCP in the range from 36.0°C to 37.25°C and deteriorated RCP out of this range (Zhu et al., 2023a).

With the advancements in non-invasive neurophysiological measurement, particularly in electrocardiogram (ECG) (Zhu et al., 2023b), functional near-infrared spectroscopy (fNIRS) (Pan et al., 2019), eye tracking (Tran et al., 2017), electroencephalogram (EEG) (Kim et al., 2020), electromyography (EMG) (Malmo and Malmo, 2000), and electrodermal activity (EDA) (Visnovcova et al., 2016), it is now possible to investigate the process and mechanism of performance impairment under severe heat stress with greater insight. Higher heart rate (Abbasi et al., 2020; Chen et al., 2020), a higher ratio of low frequency to high frequency (LF/HF) of ECG signals (Lan et al., 2010; Abbasi et al., 2020), and a decrease in pNN50 (percentage of successive RR intervals that differ by more than 50 milliseconds) (Chen et al., 2020) were noted with increased exposure to the hot-humid environment, associated with more intense activity in the autonomic nervous system and worse regulation capability of cardiovascular system. Lower peak amplitudes of the P300 component

(Nakata et al., 2021) and lower theta-band EEG (Lan et al., 2010) revealed the impairment of neural activity and lower motivation in cognitive function under heat stress. The pupil diameter is positively correlated with fatigue level and was minimized at 24°C and 40% relative humidity, while the minimized standard deviation of pupil diameter indicated an optimal concentration level (Liu et al., 2021). Several brain regions were suppressed by passive hyperthermia, including the bilateral motor cortex and left lateral-occipital cortex (compromised visual processing) (Tan et al., 2023). However, enhanced activation was reported in some other regions, such as the right superior frontal gyrus, temporal lobe, and right intra-parietal sulcus (Liu et al., 2013; Jiang et al., 2013). The hyperthermia effect on the dorsolateral prefrontal cortex (DLPFC), which is a vital brain region related to executive functions, working memory, cognitive control, and emotion regulation, remains controversial. Some studies reported enhanced activity (Liu et al., 2013; Jiang et al., 2013), while others reported decreased activity (Qian et al., 2020). Furthermore, the reduced functional connectivity within the default mode network provides another insight into the impairment of executive control performance (Qian et al., 2020).

Previous studies have extensively explored the qualitative relationship between heat strain and performance, as well as the potential biological indicators that varied with heat stress and their possible biological explanation. However, there are still research gaps. Most research has focused on temperatures below 35°C WBGT or 38°C and lacks evidence under extreme conditions encountered in serious disasters. Furthermore, there is still a lack of research on mechanisms supported by multi-physiological measurement methods.

Therefore, this work aims to investigate the effect of extreme heat stress on operators' performance and typical cognitive abilities required to deal with emergencies, such as situation awareness and work memory. Moreover, flexible physiological measurement methods with high reliability and validity including ECG, fNIRS, and eye tracking were employed to understand the mechanism underlying performance impairment. The rest of the paper is organized as follows. Section 2 illustrates the experiment, including major tasks, psychological measurements (situation awareness, working memory, and workload), and physiological measurements (fNIRS, ECG, and eye tracking), along with their data analysis methods applying neuroscience domain knowledge. In section 3, t-tests, analysis of variance, ECG signal time spectrums, task-related fNIRS signal activation analysis, rest-stating fNIRS signal functional connectivity analysis, and eye-tracking data heat map analysis were conducted to investigate the impact of hot-humid exposure on cognitive functions and human performance. In section 4, the physiological and psychological mechanisms of impaired cognitive functions under intense heat stress were discussed. The neural activity (ECG), energy metabolism (fNIRS), and visual search patterns (eye tracking) were explored, providing a neurophysiological basis for the modified maximal adaptability model. In section 5, the

limitations and contributions are discussed.

2 METHODOLOGY

2.1 Approach

In the climate lab, thirty participants were exposed for a total of 120 minutes (30 minutes \times 4) under four different conditions: 25°C 60% RH (21.26 °C WBGT), 30°C 70% RH (26.88 °C WBGT), 35°C 80% RH (31.92 °C WBGT), and 40°C 90% RH (36.81 °C WBGT). The participants' performance was recorded during major tasks, including typical NPPs (nuclear power plants) monitoring, checking, and operating tasks extracted from classic NPPs operators' cognitive model. Cognitive abilities were measured by response tasks objectively and by self-rating questionnaires subjectively. Physiological activities were recorded in real-time using an fNIRS device, eye-tracking glasses, and an ECG device placed on the participant's forehead, eyes, and chest respectively. The experimental design is shown in Figure 1.

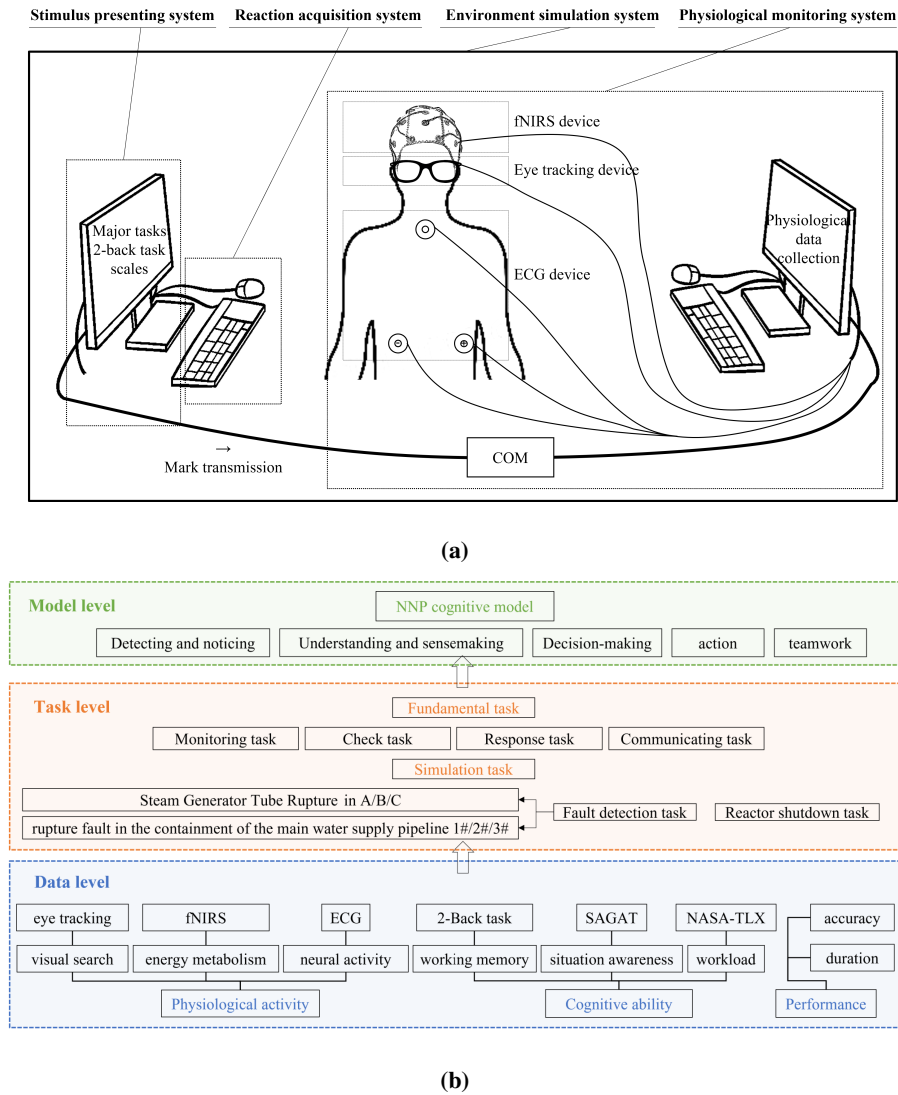


Figure 1. Illustration of experimental design. (a) schematic diagram of the experiment setup. The environment simulation system regulates temperature and humidity to achieve the desired WBGT. The stimulus presentation system displays NPPs fault detection tasks, response tasks, and questionnaires that participants interact with. The reaction acquisition system collects performance data including mouse and keyboard input. The physiological monitoring system contains an fNIRS device (on the forehead), an eye-tracking device (glasses), an ECG device (on the chest), and a computer that collects physiological data and markers from the stimulus computer via COM. (b) outline of the experiment. The experimental method includes three levels from macroscopic to concrete: model level, task level, and data level. The model level summarizes cognitive processes and typical abilities operators need. The task level sets fundamental tasks that cover elements mentioned in the model level and selects typical NPPs tasks corresponding to those fundamental tasks. The data level seeks specific methods and indicators from tasks to quantify performance, cognitive ability, and physiological activity reflecting operators' mental state.

2.2 Subjects

Thirty volunteers (16 females and 14 males) participated in this experiment, aged 20-39 years (mean: 26 ± 5 years). Prior to the experiment, all subjects were well-trained and tested to minimize the effects of practice. They were instructed to refrain from consuming caffeine and to get sufficient sleep the night before. Informed consent was obtained from all participants.

2.3 Experimental environment

To simulate a high temperature and humidity environment caused by emergencies, the experiment was implemented in the constant temperature and humidity laboratory, which is capable of adjusting the temperature within the range of 20°C to 80°C ($\pm 0.8^{\circ}\text{C}$) and the humidity within the range of 30% to 95% ($\pm 5\%$). Additionally, it provides a working space measuring $6\text{m} \times 5\text{m} \times 4.7\text{m}$.

In this experiment, we intended to explore the coupling effect of high temperature and high humidity on NPPs operators' performance. Therefore we selected the wet bulb globe temperature index (WBGT) as the independent variable. WBGT is an estimation of the heat stress on workers (for [Standardization, 2017](#)), which has been widely used as a guideline to determine appropriate work intensity for operators in hot and humid conditions. The experiment consists of four conditions and the parameters of each condition are shown in [Table 1](#).

Table 1. Condition parameters

Condition	Ta($^{\circ}\text{C}$)	RH(%)	WBGT ($^{\circ}\text{C}$)
1	25	60	21.26 ± 0.40
2	30	70	26.88 ± 0.85
3	35	80	31.92 ± 0.41
4	40	90	36.81 ± 0.89

2.4 Major task

According to NPPs operators' cognitive model ([O'Hara et al., 2008](#); [Whaley, 2016](#)), detecting and noticing, understanding and sensemaking, decision-making, action, and teamwork are the five essential cognitive and executive functions that operators require. To evaluate these essential functions, we designed four fundamental tasks: monitoring, checking, responding, and communicating respectively.

In the specific NPPs scenario, two kinds of fault detection tasks were selected: SGTR (Steam Generator Tube Rupture) (fault1) and rupture fault in the containment of the main water supply pipeline (fault2). These tasks encompass monitoring, checking, and communicating. The executive task of reactor shutdown was selected to cover checking, responding, and communicating.

To simulate NPPs operators' tasks under emergencies, we developed a virtual central control room software based on the MATALB app designer. Fault detection tasks and reactor shutdown task were implemented in the software. Subjects were asked to complete three major tasks according to the emergency plan as quickly and accurately as possible in the software. Meanwhile, duration, accuracy, error counts, fault detection time, and fault confirmation time were recorded automatically to assess the operators' performance.

- Major task 1: detect fault1 and confirm the fault type and location.
- Major task 2: detect fault2 and confirm the fault type and location.
- Major task 3: confirm the key parameters and shut down the reactor.

2.5 *Psychological measurement*

To investigate operators' mental state and cognitive ability in the task under emergencies, situation awareness, working memory, and workload were measured.

2.5.1 *Situation awareness (SA)*

SA reflects operators' perception of vital parameters, the state of key controllers, and their comprehension of the NPPs operating state at any given time. It also includes the projection of the vital systems' status in the near future. An operator with good SA can confirm faults and respond to emergencies quickly, thereby avoiding additional losses. SAGAT (Endsley, 1988) (Situation Awareness Global Assessment Technique) has been widely used to measure SA which has demonstrated good reliability and validity. SAGAT questions in this experiment were selected as:

- Perception
 - Write the approximate range of vital parameters (pressure, temperature, flow, liquid/material level, etc.)
 - Write the state of the key controller (lamp, switch, valve, pump, etc.)
- Comprehension

- Judge the status of key equipment (reactor, primary circuit, secondary circuit, steam generator, steam turbine, etc.)
- Judge the status of key systems (coolant injection system, auxiliary water supply system, etc.)
- Judge the occurring accident and locate the fault.
- Projection
 - Predict whether key equipment and systems can work after the accident.
 - Predict how would the status change after intervention.

2.5.2 Working memory

When emergencies occur, NPPs operators must process an enormous information flow. They need to extract crucial details and temporarily store them in working memory, which is an important brain executive function. Working memory was measured by a 2-back task developed by psychtoolbox3 in MATLAB. A continuous sequence of letters was displayed on the screen, and the subjects should press the arrows on the keyboard based on the comparison of each letter with the previous second one (same-left, different-right) (Figure 2). The task lasted for 3 minutes and included 30 trials.

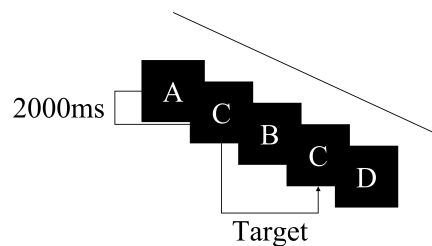


Figure 2. The experiment flow for 2-back working memory task

2.5.3 Workload

The workload can be divided into two aspects: physiological load and mental load. There is an inverse U relationship between performance and workload. Operators might become bored and not alert in emergencies when the workload remains at a low level for a long time. However, they might also find it difficult to concentrate on the major task when their remaining cognitive resource has been consumed quickly due to prolonged workload. The NASA task load index (NASA-TLX) scale was applied to assess operators' workload subjectively including mental demand, physical demand, temporal demand, performance, effort, and frustration.

2.6 Physiological measurement

2.6.1 ECG

ECG signal was recorded by a 3-lead ECG module (BIOPAC MP160, BIOPAC Systems Inc., Santa Barbara, CA), which provides information about the regulation of the cardiovascular system by neurohumoral factors and reflects the balance of activity intensity between the sympathetic and vagal nerves.

2.6.2 fNIRS

fNIRS is a non-invasive neuroimaging method that measures blood oxygenation, that reflects the energy metabolism of specific brain areas. High hemoglobin concentration (HBO) is typically associated with activation of brain regions. The prefrontal cortex (PFC) is an important brain region associated with various executive functions that we are interested in, including cognition, decision-making, and working memory. An 8-channel fNIRS device (Artinis Octamon, Netherlands) was placed on the PFC to measure brain activity, with the probe placement shown in Figure 3 and Table 2. In addition, the NIRS-KIT toolbox (Hou et al., 2021) was utilized to assist in processing the fNIRS data partly.

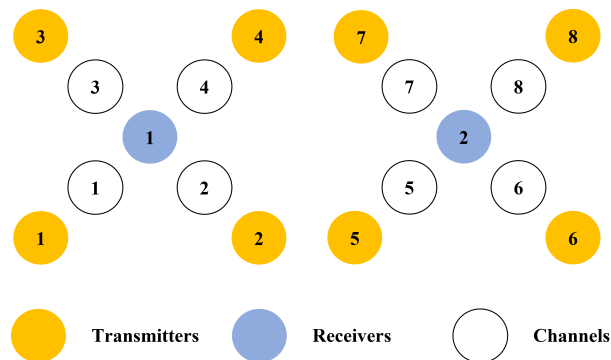


Figure 3. fNIRS probe placement

Table 2. Localization of fNIRS channels and their corresponding Brodmann areas.

channel	Brodmann area
ch1	10 - Frontopolar area
	46 - Dorsolateral prefrontal cortex
ch2	10 - Frontopolar area
ch3	45 - pars triangularis Broca's area
	46 - Dorsolateral prefrontal cortex
ch4	9-46 - Dorsolateral prefrontal cortex
	10 - Frontopolar area
ch5	10 - Frontopolar area
	46 - Dorsolateral prefrontal cortex
ch6	45 - pars triangularis Broca's area
	46 - Dorsolateral prefrontal cortex
ch7	9-46 - Dorsolateral prefrontal cortex
	10 - Frontopolar area
ch8	45 - pars triangularis Broca's area
	46 - Dorsolateral prefrontal cortex

2.6.3 Eye Tracking

Eye tracking data was obtained by Dikablis Glass 3 to observe the distribution of participants' attention during tasks. This allowed the exploration of operators' virtual search patterns in hot and humid environments. Prior to each condition, eye movement calibration was performed.

2.7 Procedure

The study involved four different WBGT conditions, and each consists of nine phases: baseline rest (P1), completion of major task1 and answering SAGAT questions (P2-3), completion of major task2 and answering SAGAT questions (P4-5), completion of major task3 and answering SAGAT questions (P6-7), answering the NASA-TLX scale (P8), completion of the 2-back task (P9), recovery while waiting for temperature and humidity to reach the target, and looping through all the phases again until the tasks in all the conditions were completed. The major tasks were outlined in §2.4 but their order was randomized.

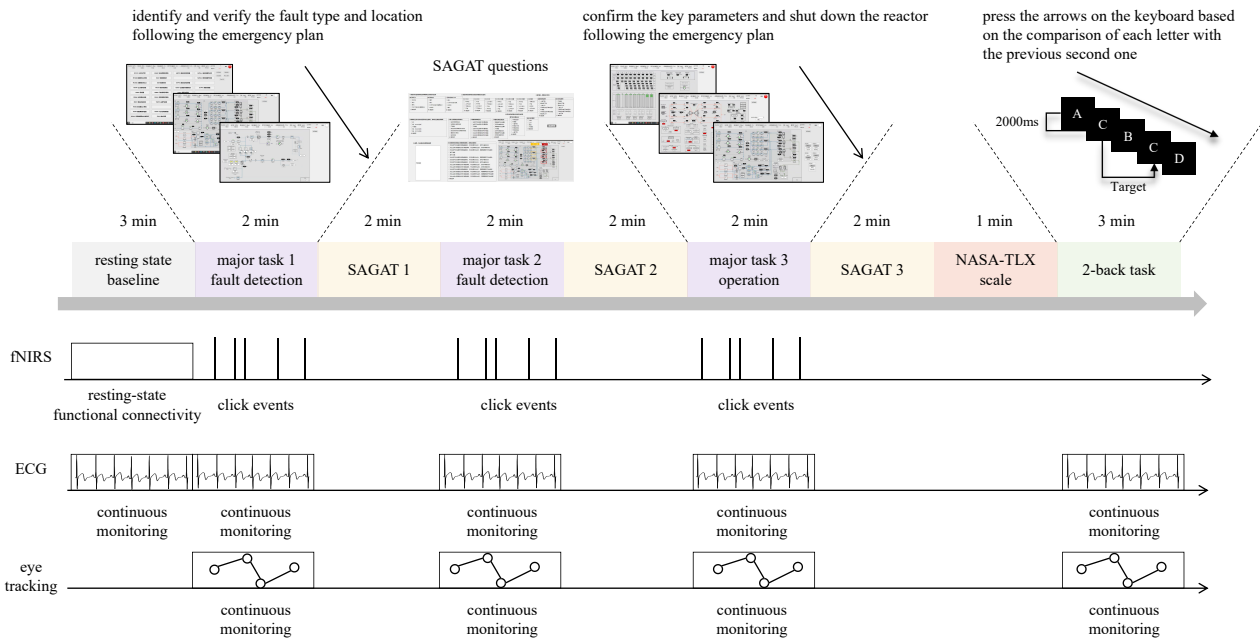


Figure 4. Experiment procedure in every condition. Each phase lasted for 5 minutes.

2.8 Data analysis

2.8.1 Performance and psychological measurement data

Performance and psychological data were recorded by the developed software mentioned in §2.4 automatically, and the extracted features for each task are listed in Table 3.

The difference of each feature for each subject was calculated between adjacent conditions (condition 1 and 2, 2 and 3, 3 and 4). One sample t-test was performed to determine any significant difference from 0.

Table 3. Performance and psychological measurement features

performance	Situation awareness	workload	Work memory
task completion rate [%]	SAGAT completion time [s]	mental demand score	number of correct responses [n.u.]
error numbers [n.u.]	total score	physical demand score	number of wrong responses [n.u.]
fault detection time [s]	level1 perception score	temporal demand score	number of missed responses [n.u.]
fault confirmation time [s]	level2 comprehension score	performance score	mean reaction time of all responses [s]
completion time [s]	level3 projection score	effort score	standard deviation of all response reaction times [s]
	communication score	frustration score	mean reaction time of all correct response [s]
		total score	standard deviation of all correct response reaction times [s]

2.8.2 ECG and HRV

Time domain analysis. Signal filtering and the QRS complex detection were applied to extract the RR interval series. From these series, various characteristic features were calculated and summarized in Table 4. Analysis of variance (ANOVA) was performed on each feature to identify significant differences between any two conditions.

Frequency domain analysis. The fast Fourier transform (FFT) was applied to the filtered ECG data to calculate its power spectral density (PSD). Spectral power was calculated as the area below the PSD curve which was then divided into four frequency bands: very low-frequency power (VLF) in [0, 0.04] Hz, low-frequency power (LF) in [0.04, 0.15] Hz, high-frequency power (HF) in [0.15, 0.4] Hz and very high-frequency power (VHF) in [0.4, 3] Hz. Typical features are summarized in Table 4. ANOVA was also performed on the frequency features.

Table 4. ECG features in time domain and frequency domain.

Domain	ECG features	Unit	Description
Time domain	RR interval	[s]	Average of time distance between two adjacent R peaks
	HR	[bpm]	Numbers of heart beat every minute
	R amplitude	No unit	R wave peak amplitude
	P amplitude	No unit	P wave peak amplitude
	QRS width	[s]	Time between onset and end of the QRS complex
	PRQ width	[s]	Time between onset of the P wave to the Q wave
	QT interval	[s]	Time between the beginning of the Q wave and the end of the T wave
	QTC interval	[s]	QT time interval divided by the square root of the RR interval
	ST interval	[s]	Time between the S wave to the end of the T wave
	SDNN	[s]	Standard deviation of RR time series
	RMSSD	[s]	Root mean square of the difference of all subsequent RR intervals
	SDSD	[s]	Standard deviation of the difference of all subsequent RR intervals
	PNN50	%	Percentage of RR intervals in which the change of successive NN exceeds 50 ms
	Frequency domain	VLF	[s ²]
LF		[s ²]	Spectral power of the RR time series in the band [0.04; 0.15 Hz]
HF		[s ²]	Spectral power of the RR time series in the band [0.15; 0.4 Hz]
VHF		[s ²]	Spectral power of the RR time series in the band [0.4; 3 Hz]
Sympathetic-vagal balance		No unit	Ratio between LF and HF
Sympathetic		No unit	Ratio between LF and (VLF+LF+HF)
Vagal	No unit	Ratio between HF and (VLF+LF+HF)	

Time-frequency domain analysis. The ECG data was a non-stationary signal in every task and condition. Therefore, all ECG data was scaled to [0, 100%] on the timeline to obtain the same-length ECG data and the Short-time Fourier Transform (STFT) with [0, 3Hz] frequency limits, 0.5 frequency resolution, 20% overlapping, 0.875 leakage function was applied on the filtered ECG to get time spectrogram. Time-frequency representation of the RR time series provides valuable insights into the changes in frequency components and energy distribution over time.

2.8.3 fNIRS

Raw fNIRS data contains several types of noise. Thus, the fNIRS signal was bandpass filtered between 0.01Hz and 0.1Hz to eliminate 50Hz noise as well as most physiological noise. First detrending was implemented to prevent baseline drift. Motion correction was then applied to mitigate motion artifacts. Following preprocessing, a general linear model analysis was conducted to plot the PFC activation map and identify valid activated brain regions under tasks. Additionally, functional connectivity analysis was conducted on the resting-state fNIRS data to explore brain synchrony in different conditions.

General linear model (GLM) activation analysis. Beta values were derived by regressing the HBO curve against the reference curve, which was obtained by convolving the click event list with the HRF function. A one-sample t-test (different from 0) was performed on the betas to figure out the activated channels in the PFC.

Resting-state functional connectivity (FC) analysis. The correlation coefficient (CORR), correlation coefficient after fishier-Z transformation (CORR fisher-Z), coherence (COH), and phase-locking value (PLV) were calculated between different channels. The results were corrected by multiple comparisons using NBS and a functional connectivity matrix was generated.

The correlation coefficient between the signal x and y is calculated by the following formula:

$$R_{xy} = \frac{1}{N} \sum_{k=1}^N x(k)y(k) \quad (1)$$

Coherence is calculated by the following formula, in which $S_{xy}(f)$ is cross-power spectral density between signal x and y at frequency f , $S_{xx}(f)$ and $S_{yy}(f)$ are auto-power spectral density for signal x and y at frequency f respectively.

$$\text{COH}_{xy} = |K_{xy}(f)|^2 = \frac{|S_{xy}(f)|^2}{S_{xx}(f)S_{yy}(f)} \quad (2)$$

Phase-locking value is calculated by the following formula, in which $\Delta\phi_{rel}(t)$ is the phase difference between the

complex signal \tilde{x} and \tilde{y} obtained by the Hilbert transform.

$$PLV = |\langle e^{i\Delta\phi_{rel}(t)} \rangle| = \left| \frac{1}{N} \sum_{n=1}^N e^{i\Delta\phi_{rel}(t_n)} \right| = \sqrt{\langle \cos \Delta\phi_{rel}(t) \rangle^2 + \langle \sin \Delta\phi_{rel}(t) \rangle^2} \quad (3)$$

2.8.4 Eye tracking

AOI and pupil analysis. 6 pages of interest and 9 areas of interest (AOIs) were set up (shown in Figure 5) to collect eye-tracking related features (listed in Table 5) which can reflect information search efficiency, information processing efficiency, mental load, and concentration. The difference of each feature in each subject was calculated between the adjacent conditions (condition1 and 2 , 2 and 3, 3 and 4). One sample t-test was performed to identify a significant difference from 0.

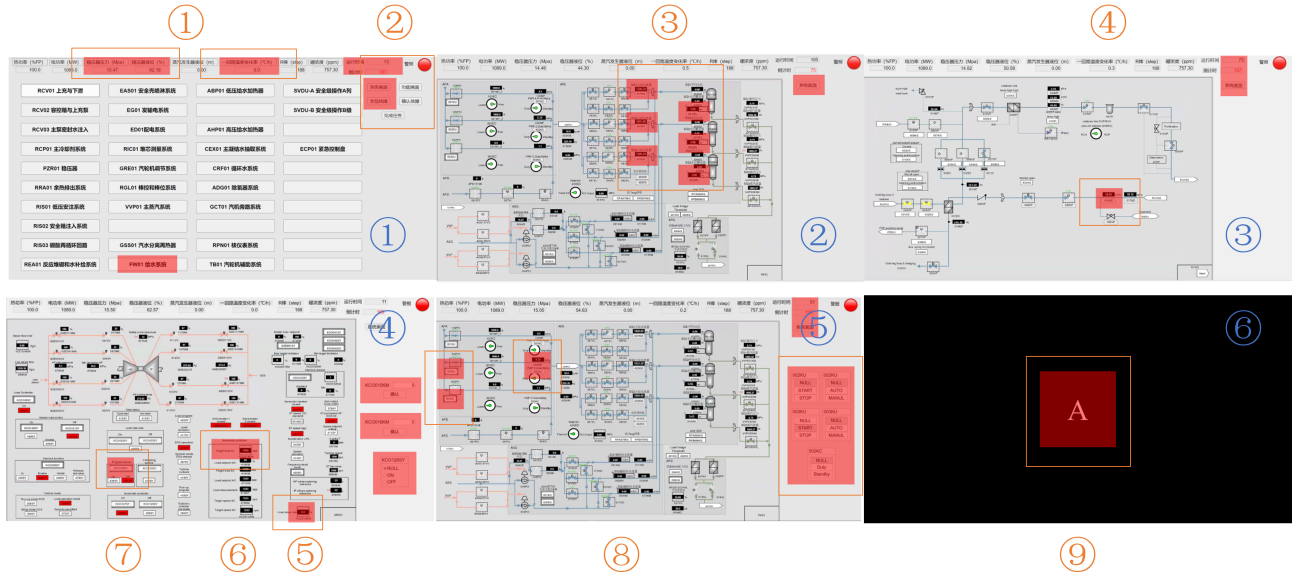


Figure 5. AOIs settings. Red areas are AOIs that cover important information that operators should monitor, check, or control.

Table 5. Eye-tracking related features

Domain	Feature	Unit	Description
AOI related	Number of glances>2s	No unit	The number of single glance more than 2 seconds
	Total Glance time	[s]	Total glance time on a specific AOI
	Mean Glance Duration	[s]	Average duration of each glance, total glance time / number of glances
	Glance Rate	[1/s]	The number of glances on a AOI every second
	AOI Attention Ratio	[%]	Glance time on a specific AOI / task duration
	Vertical Eye Activity	[pixel]	Standard deviation of y coordinates in the screen
	Mean fixation duration left	[ms]	Average fixation duration of left eye in an AOI
	Mean fixation duration right	[ms]	Average fixation duration of right eye in an AOI
	Number of saccades right	No unit	Total number of saccades of right eye in an AOI
Task and pupil related	Duration	[s]	Duration on an interest page
	Percentage Transition Times	[%]	Time of transiting between different AOIs / duration
	Pupil left avg		Average pupil diameter of left eye
	Pupil right avg		Average pupil diameter of right eye

Heat map analysis. The heat map was created on 6 pages of interest, displaying a deeper color (red) in areas with more glances and a lighter color (green) in areas with fewer glances. This visualization effectively reflects the distribution of attention.

3 RESULTS

3.1 Task performance and cognitive ability

One sample t-test (differ from 0) was applied among all the features across adjacent conditions. All the significant p values are shown in Table 6 and visualized as boxplots with average lines in Figure 6. Statistical significance is accepted at $p < 0.05$.

3.1.1 Task performance

Statistic results indicated that for task complement rate, no significant difference was observed between different conditions. Operators can follow all the necessary steps even in a hot and humid environment.

In the monitor and check task, the number of misoperations showed no significant result, however in the response task

did (between condition 2 and 3, $t = 2.59, p = 0.02$). It suggested that monitor and check ability was less affected by temperature and humidity. Workers were more likely to make mistakes at around 32°C WBGT (condition 3).

In the monitor and check task, fault detection time in condition 2 was significantly less than condition 1 ($t = -2.11, p = 0.05$), as well as fault confirmation time ($t = -3.19, p < 0.01$).

In response task, task completion time in condition 4 was significantly less than condition 3 ($t = -3.14, p < 0.01$), and in condition 2 is significantly less than condition 1 ($t = -2.08, p = 0.05$).

3.1.2 *Situation awareness*

As for the total SA score, the score in condition 4 was significantly lower than condition 3 ($t = -2.31, p = 0.03$).

For more detail, in terms of level 1 SA perception, there was no significant difference between different conditions and tasks. It indicated that perception is a low-level situation awareness ability that was less affected by the environment. As for level 2 SA comprehension, there was a significantly lower score in condition 3 than 2 in the response task ($t = -2.43, p = 0.02$). As for level 3 SA projection, there was also no significant difference between conditions and tasks. Regarding communication, the score in condition 4 was significantly less than condition 3 ($t = -2.13, p = 0.04$).

3.1.3 *Workload*

In the NASA-TLX scale, physical demand had a significant increase from condition 2 to condition 4 ($t = 2.66, p = 0.01$ and $t = 5.99, p < 0.01$). Temporal demand in condition 2 was greatly less than condition 1 ($t = -2.27, p = 0.03$). Effort score in condition 4 was greatly higher than condition 3 ($t = 2.25, p = 0.03$). The task load index total score in condition 2 was greatly less than condition 1 ($t = -2.27, p = 0.03$). Moreover, no significant difference was observed in mental demand, performance, and frustration between different conditions.

3.1.4 *Work memory*

In the 2-back task, no great difference was shown in the number of correct responses and wrong responses, but the missed number in condition 2 was greatly less than condition 1 and condition 3 ($t = 0.73, p = 0.01$ and $t = -2.81, p = 0.02$). The mean reaction time of all correct responses in condition 4 was significantly less than condition 3 ($t = -3.69, p < 0.01$).

Table 6. The summary of significant results in performance, situation awareness, workload, and work memory. Values are presented as median \pm standard deviation. Bold values indicate significant results with a p-value less than 0.05 or less than 0.01. Values in task: 1 means monitoring and check task, 2 means response task, / means average all tasks.

Feature	Task	C1	C2	C3	C4	p C2-C1	p C3-C2	p C4-C3
Performance								
error counts	2	4.00 \pm 6.91	3.41 \pm 5.65	4.78 \pm 6.95	2.89 \pm 2.47	0.21	0.02	0.10
fault detection time	1	3.71 \pm 2.20	2.82 \pm 1.13	3.03 \pm 1.41	3.14 \pm 2.12	0.05	0.37	0.27
fault confirm time	1	33.33 \pm 14.35	28.65 \pm 12.65	26.67 \pm 10.99	25.35 \pm 8.68	<0.01	0.18	0.91
completion time	/	82.76 \pm 37.41	73.64 \pm 31.12	70.91 \pm 23.18	61.54 \pm 18.38	0.05	0.37	<0.01
Situation awareness								
Total score	1	82.59 \pm 21.14	81.85 \pm 24.07	86.30 \pm 18.94	80.37 \pm 26.31	0.82	0.18	0.03
comprehension	2	23.33 \pm 4.16	23.89 \pm 3.49	22.96 \pm 3.74	23.70 \pm 2.97	0.08	0.02	0.16
communication	1	4.44 \pm 1.60	4.07 \pm 1.98	4.63 \pm 1.33	3.89 \pm 2.12	0.33	0.08	0.04
Workload								
physical demand	/	23.68 \pm 19.11	24.18 \pm 17.50	30.17 \pm 20.14	43.56 \pm 22.81	0.56	0.01	<0.01
temporal demand	/	43.74 \pm 22.57	38.26 \pm 19.44	38.37 \pm 22.16	41.73 \pm 22.06	0.03	0.97	0.16
effort	/	44.63 \pm 23.86	39.08 \pm 22.10	40.93 \pm 22.00	46.94 \pm 22.32	0.09	0.33	0.03
total score	/	48.40 \pm 29.30	42.78 \pm 22.55	43.42 \pm 23.50	46.47 \pm 22.35	0.03	0.72	0.09
Work memory								
missed number	/	0.62 \pm 0.90	0.27 \pm 0.53	0.73 \pm 0.96	0.92 \pm 2.56	0.01	0.02	0.73
mean reaction time of correct responses	/	1.12 \pm 0.18	1.10 \pm 0.16	1.07 \pm 0.17	1.02 \pm 0.16	0.39	0.19	<0.01

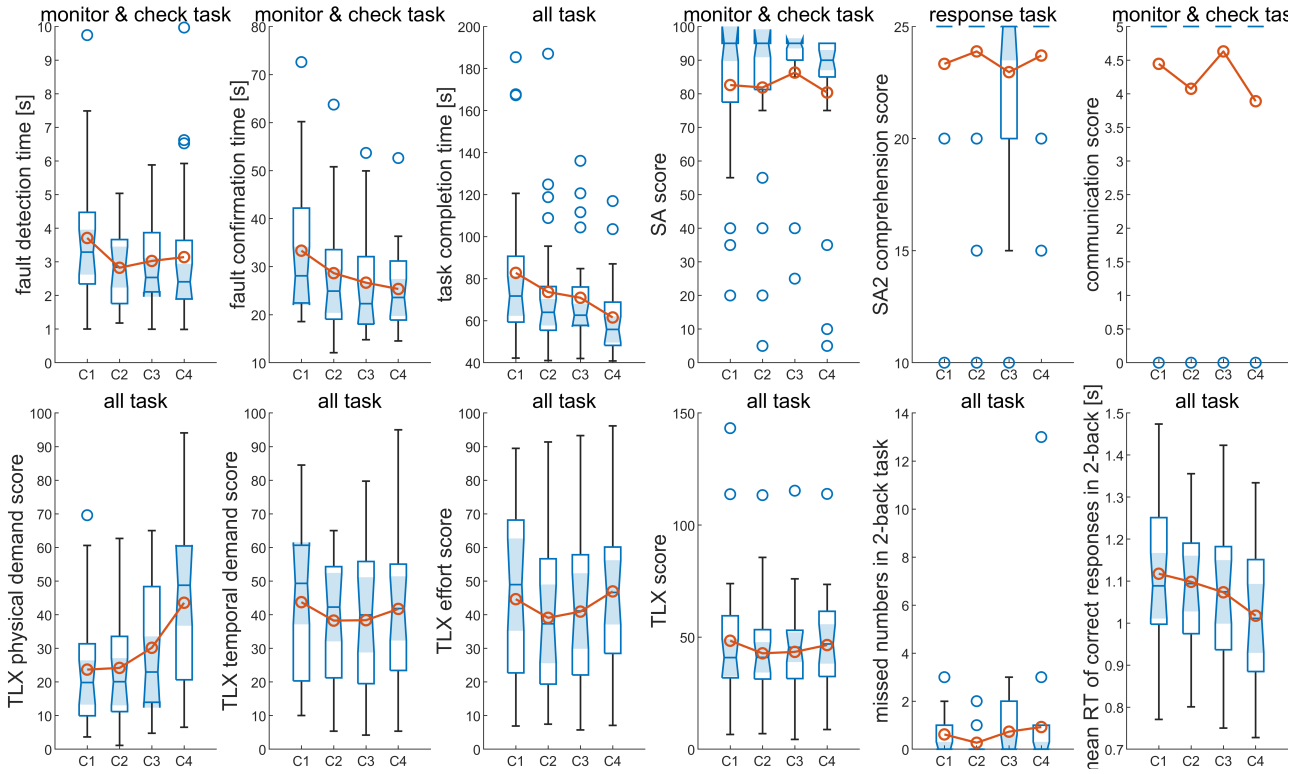


Figure 6. The boxplots display significant results in performance, situation awareness, workload, and work memory. Red lines represent average values.

3.2 Physiological measurement results

3.2.1 ECG and HRV

ANOVA was applied among all the ECG features across adjacent conditions. All the significant p values are shown in Table 7 and visualized as boxplots with average lines in Figure 7. Statistical significance is accepted at $p < 0.05$.

Time domain. RR interval and ST interval in condition 4 were greatly less than condition 1-3 ($F = 27.64, p < 0.01$ and $F = 4.28, p = 0.02, 0.01, 0.04$). And QT interval in condition 4 was greatly shorter than condition 1-2 ($F = 3.86, p = 0.03, 0.02$). HR in condition 4 was greatly faster than condition 1-3 ($F = 29.46, p < 0.01$). Furthermore, SDNN, RMSSD, SDSD, and PNN50 in condition 4 were greatly less than condition 1-2 ($F = 5.76, p \leq 0.01$ and $F = 8.37, p < 0.01$ and $F = 8.34, p < 0.01$ and $F = 7.96, p < 0.01$). RMSSD, SDSD, PNN50 in condition 3 were significantly less than condition 1 ($F = 8.37, p = 0.01$ and $F = 8.34, p = 0.01$ and $F = 7.96, p = 0.02$).

Frequency domain. LF/HF in condition 3-4 was greatly more than condition 1 ($F = 5.45, p \leq 0.01$). Vagal in condition 3-4 was greatly less than condition 1 ($F = 6.44, p < 0.01$).

Time-frequency domain. As shown in Figure 8, a frequency band could be found around 1.5 Hz. PSD of the frequency band increased among different tasks and decreased in the last task. Band frequency, high-frequency component, and overall PSD increased with temperature and humidity.

Table 7. The summary of significant results in ECG features. Values are presented as median \pm standard deviation. Bold values indicate significant results with a p-value less than 0.05.

Feature	C1	C2	C3	C4	p C1-C2	p C1-C3	p C1-C4	p C2-C3	p C2-C4	p C3-C4
Time domain										
RR interval [s]	0.68 \pm 0.08	0.69 \pm 0.08	0.67 \pm 0.08	0.61 \pm 0.08	1.00	0.34	< 0.01	0.27	< 0.01	< 0.01
HR [bpm]	89.29 \pm 11.08	89.05 \pm 10.91	91.42 \pm 11.32	100.94 \pm 13.77	1.00	0.45	< 0.01	0.35	< 0.01	< 0.01
QT interval [s]	0.41 \pm 0.13	0.41 \pm 0.13	0.40 \pm 0.13	0.36 \pm 0.13	1.00	0.99	0.03	0.96	0.02	0.06
ST interval [s]	0.33 \pm 0.13	0.34 \pm 0.13	0.33 \pm 0.13	0.29 \pm 0.13	1.00	0.99	0.02	0.96	0.01	0.04
SDNN [s]	0.04 \pm 0.01	0.04 \pm 0.01	0.03 \pm 0.01	0.03 \pm 0.02	0.78	0.25	< 0.01	0.80	0.01	0.14
RMSSD [s]	0.02 \pm 0.01	0.02 \pm 0.01	0.02 \pm 0.01	0.02 \pm 0.02	0.77	0.01	< 0.01	0.16	< 0.01	0.43
SDSD [s]	0.02 \pm 0.01	0.02 \pm 0.01	0.02 \pm 0.01	0.02 \pm 0.02	0.77	0.01	< 0.01	0.16	< 0.01	0.43
PNN50 [%]	2.26 \pm 3.08	2.04 \pm 2.97	1.38 \pm 2.12	0.92 \pm 1.47	0.88	0.02	< 0.01	0.14	< 0.01	0.44
Frequency domain										
Sympathetic-vagal balance	1.84 \pm 1.41	2.38 \pm 2.08	2.79 \pm 2.36	2.89 \pm 3.30	0.24	0.01	< 0.01	0.50	0.29	0.98
Vagal	0.38 \pm 0.20	0.34 \pm 0.19	0.30 \pm 0.18	0.29 \pm 0.20	0.28	< 0.01	< 0.01	0.29	0.15	0.99

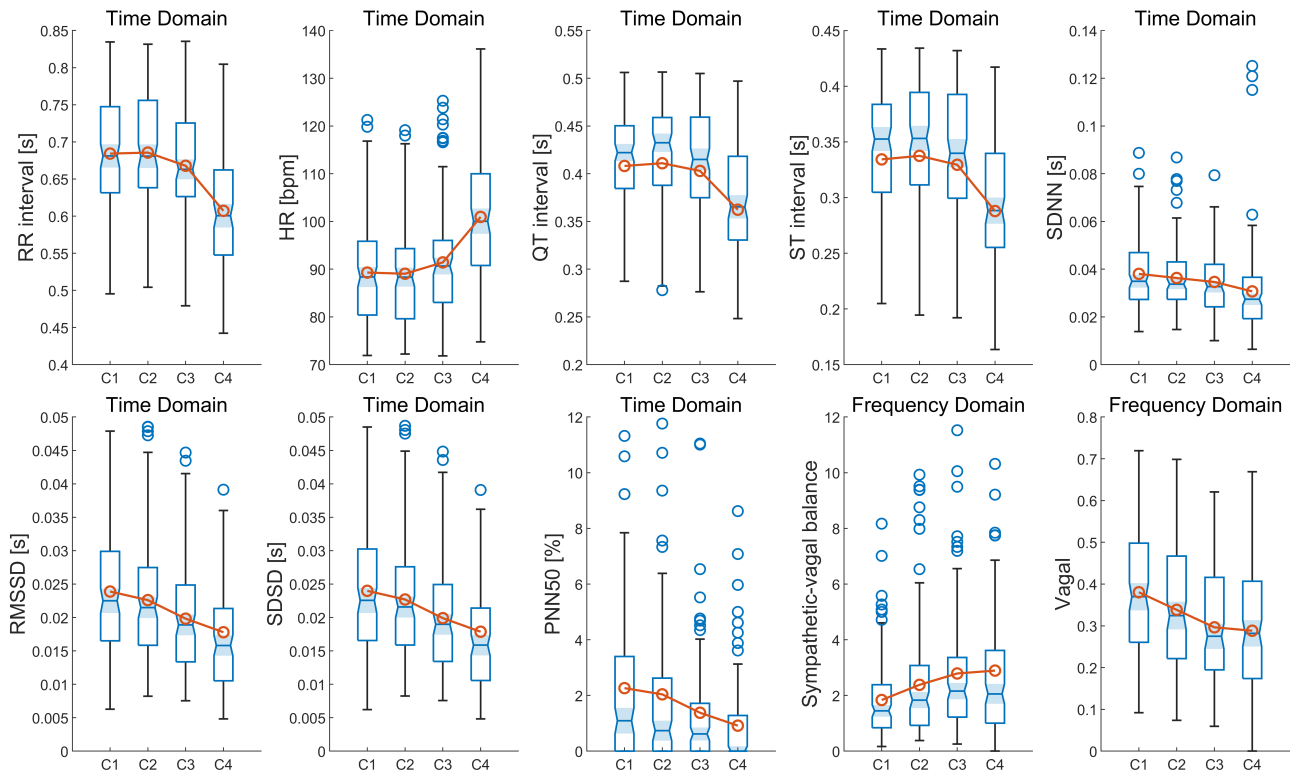


Figure 7. The boxplots display significant results in ECG features. Red lines represent average values.

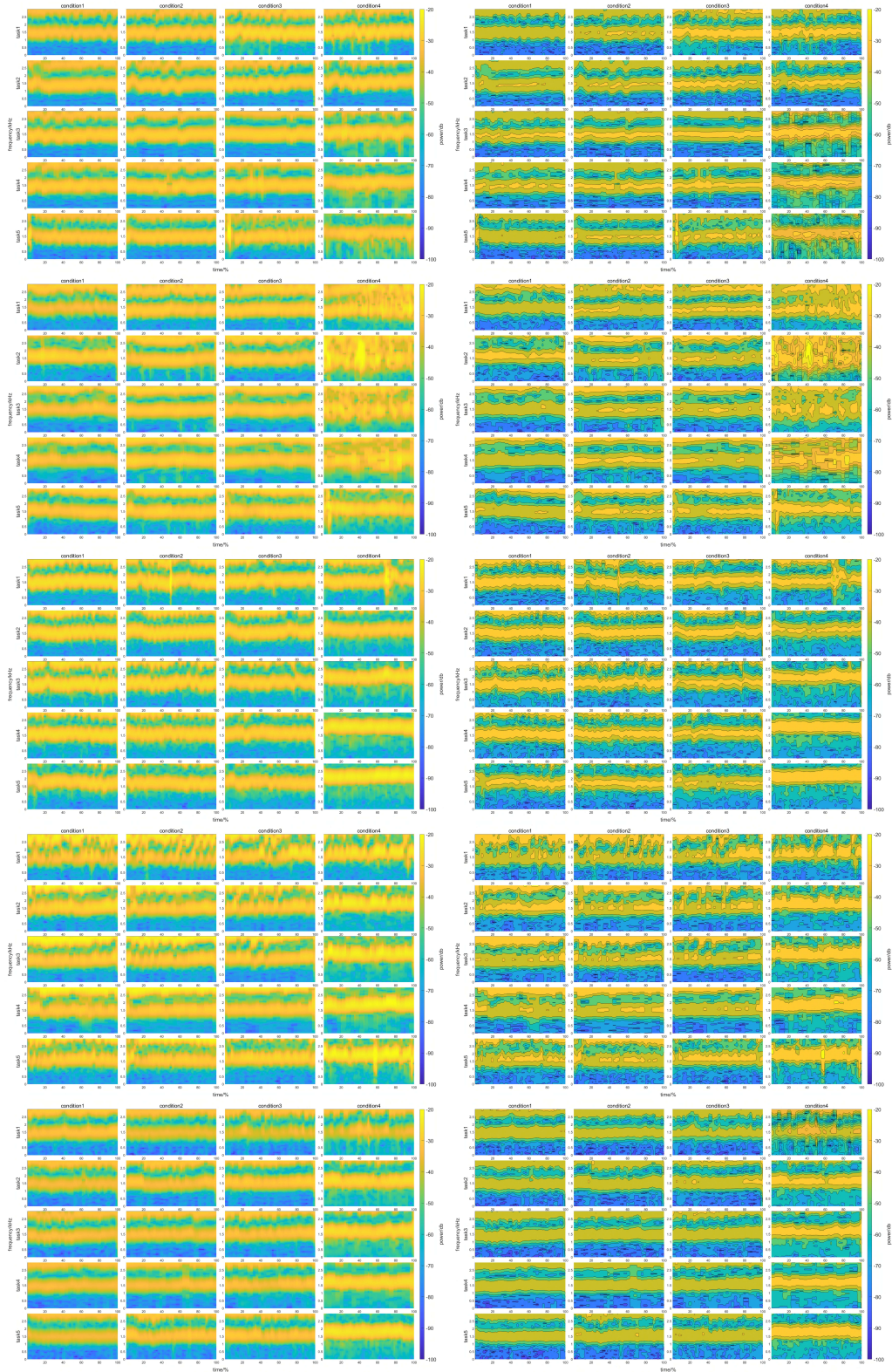


Figure 8. The typical time-frequency representation of RR time series for 9 subjects among different conditions (in columns) and different tasks (in rows). left plots are the raw time-frequency representation of the RR time series and right plots with contour lines on.

3.2.2 *fNIRS*

GLM results. One sample t-test (differ from 0) was applied among GLM betas for tasks and conditions. All the significant p values are shown in Table 8 and visualized as a PFC activation map in Figure 9. Statistical significance is accepted at $p < 0.05$. Results revealed that there was no activated channel in condition 1. In condition 2, there were 4 activated channels (ch3, ch4, ch5, ch6) in the fault detection task and 4 activated channels (ch1, ch5, ch6, ch7) in the operation task. In condition 3, there were 3 activated channels (ch4, ch5, ch6) in the fault detection task and no activated channels in the operation task. In condition 4, there was only 1 activated channel (ch5) in the fault detection task and 0 in the operation task.

Table 8. The t values for GLM betas. Bold values indicate significant results with a p-value less than 0.05. The detection task had more activated channels than the operation task. Condition 2 and 3 had more activated channels.

condition	task	Valid channels	ch1 p	ch2 p	ch 3 p	ch 4 p	ch5 p	ch6 p	ch7 p	ch8 p
25°C 60%	detection	0	0.59	0.45	0.94	0.21	0.57	0.24	0.69	0.89
	operation	0	0.19	0.69	0.83	0.66	0.65	0.93	0.62	0.97
30°C 70%	detection	4	0.21	0.15	0.04	0.00	0.02	0.00	0.69	0.06
	operation	4	0.02	0.07	0.10	0.05	0.04	0.02	0.02	0.13
35°C 80%	detection	3	0.19	0.07	0.07	0.00	0.00	0.03	0.15	0.18
	operation	0	0.96	0.46	0.38	0.72	0.88	0.94	0.76	0.66
40°C 90%	detection	1	0.97	0.92	0.46	0.15	0.02	0.13	0.86	0.28
	operation	0	0.57	0.55	0.15	0.63	0.14	0.25	0.40	0.22

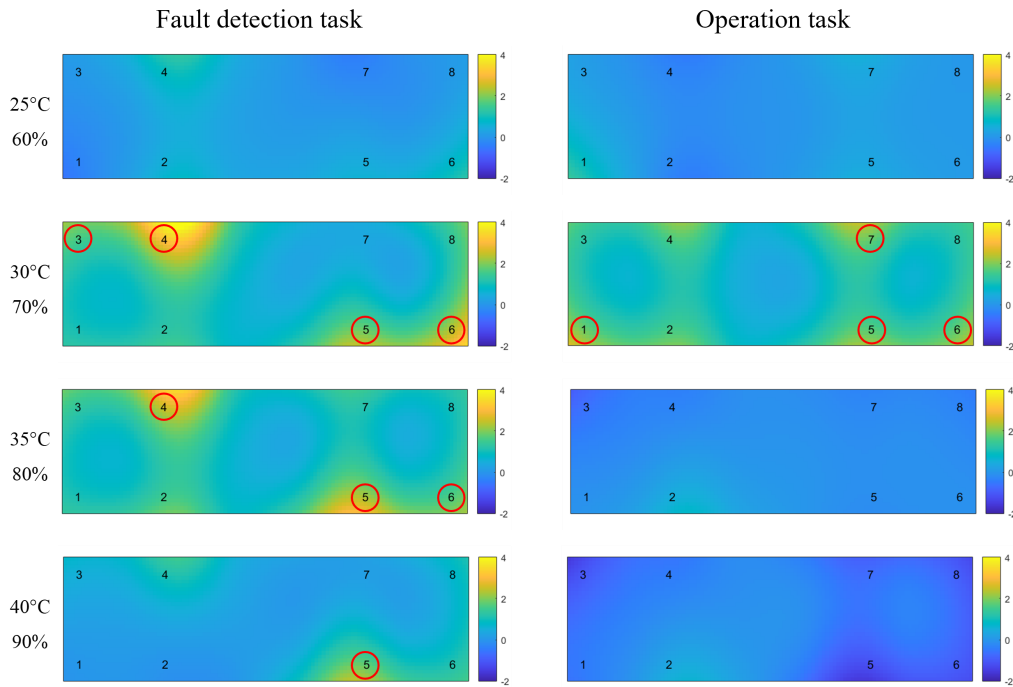


Figure 9. The PFC activation map among conditions and tasks. Red circles reveal valid activated channels (betas differ from 0)

Resting-state FC results. Four kinds of FC matrix (CORR, CORR fisher-Z, COH, PLV) were plotted in Figure 10. NBS correction (multiple comparisons correction) was applied and valid results are listed in Table 9 and plotted in Figure 11. For coherence (COH), frequency synchronization, there were great differences between condition 2 and 4 ($p < 0.01$) in ch1 and ch2 ($t = 5.08$), ch1 and ch5 ($t = 2.63$), ch2 and ch4 ($t = 2.79$), ch2 and ch6 ($t = 2.80$), ch4 and ch8 ($t = 2.71$), ch7 and ch8 ($t = 3.23$) and between condition 3 and 4 ($p = 0.03$) in ch1 and ch4 ($t = 2.81$), ch3 and ch4 ($t = 2.69$), ch4 and ch5 ($t = 3.33$). For correlation (CORR), the time synchronization, there were great differences between condition 1 and 4 ($p = 0.04$) in ch1 and ch2 ($t = 2.93$), ch1 and ch6 ($t = 3.00$), and between condition 3 and 4 ($p = 0.05$) in ch3 and ch4 ($t = 2.67$), ch4 and ch6 ($t = 2.56$). No significant difference was reported among any condition and any channel for PLV.

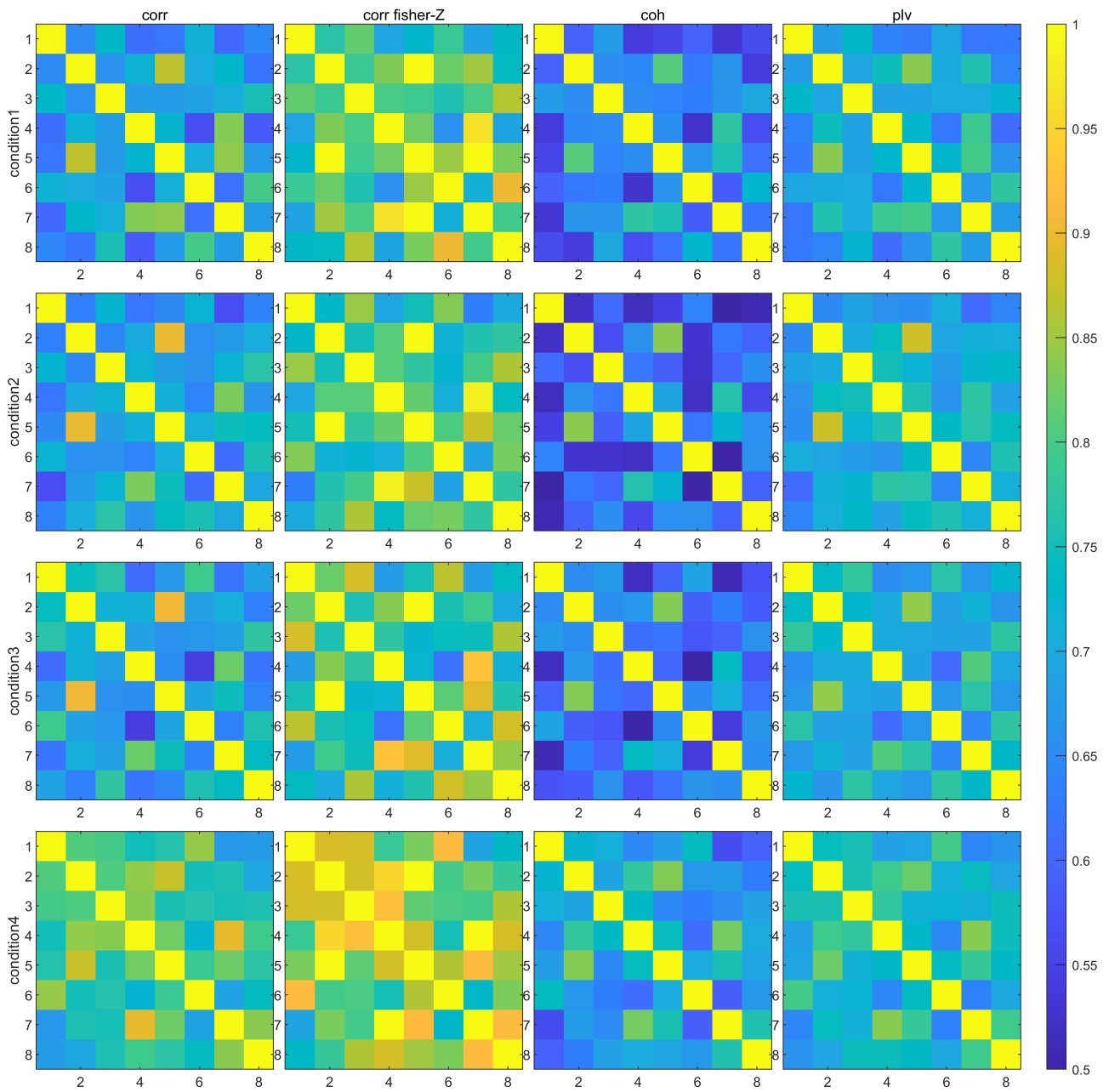


Figure 10. Four kinds of FC matrix (CPRR, CORR fisher-Z, COH, PLV) for 4 conditions.

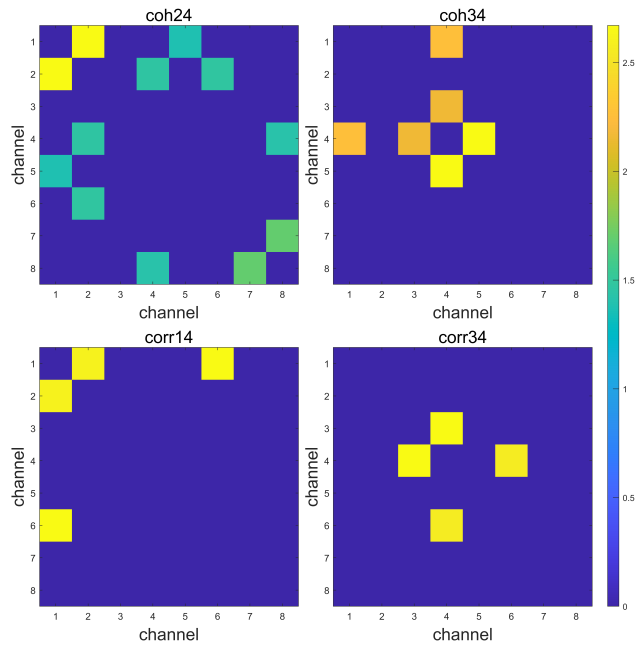


Figure 11. Valid FC matrix after NBS correction

Table 9. Valid results after NBS correction

feature	Condition1	Condition 2	Channel 1	Channel 2	t	p	
Coherence	2	4	1	2	5.08	< 0.01	
			1	5	2.63		
			2	4	2.79		
			2	6	2.80		
			4	8	2.71		
			7	8	3.23		
	3	4	1	4	2.81	0.03	
Correlation	1	4	1	2	2.93	0.04	
			1	6	3.00		
			3	4	2.67		0.05
			4	6	2.56		

3.2.3 Eye tracking

One sample t-test (differ from 0) was applied among all the eye-tracking features across adjacent conditions. All the significant p values are shown in Table 10 and Table 11 and visualized as boxplots with average lines in Figure 12 and Figure 13. Statistical significance is accepted at $p < 0.05$.

AOI results. As shown in Table 10 and Figure 12, the number of single glance more than 2 seconds in condition 3 was greatly more than condition 2 ($t = 2.18, p = 0.04$). Total glance time, mean glance duration, and AOI attention ratio in condition 3 were significantly more than condition 2 ($t = 2.21, p = 0.04$ and $t = 3.07, p = 0.01$ and $t = 2.58, p = 0.02$) and more than condition 4 ($t = -2.57, p = 0.02$ and $t = -2.28, p = 0.04$ and $t = 3.23, p < 0.01$). Glance rate, mean fixation duration and mean saccade angle right in condition 2 were greatly more than condition 1 ($t = 2.63, p = 0.02$ and $t = 2.14, p = 0.04$ and $t = 2.41, p = 0.02$). Vertical eye activity and the number of saccades right in condition 4 were more than condition 3 ($t = 2.73, p = 0.01$ and $t = 2.05, p = 0.05$). The mean fixation duration right in condition 4 was greatly less than condition 3 ($t = -2.27, p = 0.03$).

Table 10. The summary of significant results in AOI-related features. Values are presented as median \pm standard deviation. Bold values indicate significant results with a p-value less than 0.05. Values in task: 1 means monitoring task, 2 means check task, 3 means response task.

Feature	Task	C1	C2	C3	C4	p C2-C1	p C3-C2	p C4-C3
Number of glances>2s	1	0.33 \pm 0.79	0.19 \pm 0.47	0.67 \pm 1.47	0.65 \pm 1.30	0.36	0.04	0.76
Total Glance time [s]	3	1.07 \pm 0.40	1.01 \pm 0.39	1.30 \pm 0.52	1.02 \pm 0.38	0.46	0.04	0.02
Mean Glance Duration [s]	3	0.95 \pm 0.39	0.86 \pm 0.38	1.21 \pm 0.53	0.96 \pm 0.43	0.46	0.01	0.04
Glance Rate [1/s]	3	0.05 \pm 0.02	0.06 \pm 0.02	0.05 \pm 0.01	0.06 \pm 0.03	0.02	0.09	0.28
AOI Attention Ratio [%]	1	60.50 \pm 15.31	61.10 \pm 15.95	58.75 \pm 18.20	51.87 \pm 22.15	0.82	0.31	< 0.01
AOI Attention Ratio [%]	3	4.79 \pm 1.66	4.92 \pm 1.57	6.32 \pm 2.26	5.36 \pm 1.71	0.72	0.02	0.08
Vertical Eye Activity [pixel]	1	80.66 \pm 22.55	88.18 \pm 32.22	82.66 \pm 33.15	99.87 \pm 51.64	0.16	0.18	0.01
Mean fixation duration left [ms]	2	1172.75 \pm 565.56	1592.61 \pm 1014.11	1702.61 \pm 1314.78	1404.03 \pm 929.85	0.05	0.72	0.27
Mean fixation duration right [ms]	1	439.73 \pm 97.46	472.45 \pm 131.91	475.96 \pm 96.15	432.08 \pm 121.18	0.04	0.88	0.03
Mean fixation duration right [ms]	3	857.67 \pm 484.26	781.05 \pm 430.88	1039.89 \pm 676.90	664.45 \pm 392.81	0.99	0.08	0.04
Mean saccade angle right [deg]	1	3.88 \pm 1.97	4.70 \pm 0.94	4.90 \pm 0.95	4.99 \pm 1.38	0.02	0.32	0.79
Number of saccades right	1	6.93 \pm 5.17	6.94 \pm 3.60	8.03 \pm 5.40	10.62 \pm 8.37	0.67	0.30	0.05

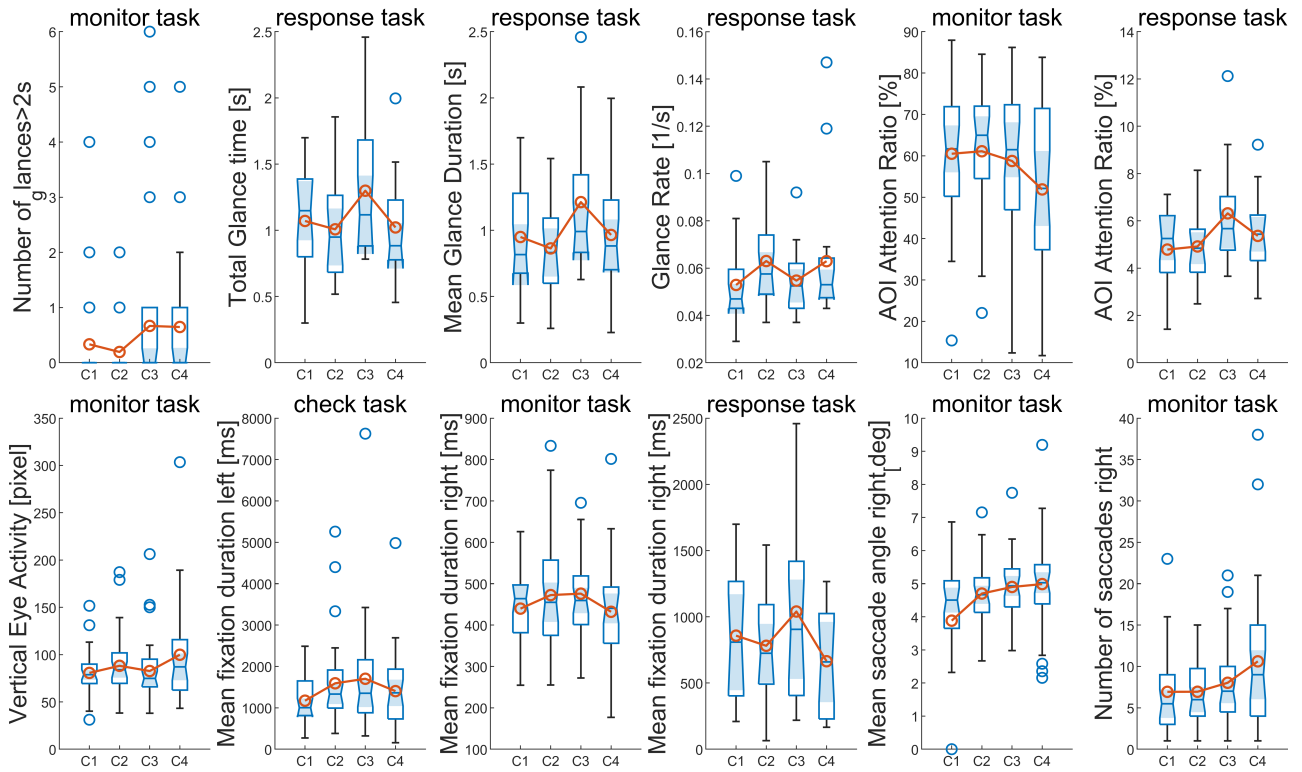


Figure 12. The boxplots display significant results in AOI-related features. Red lines represent average values.

Pupil results. As shown in Table 11 and Figure 13, duration in condition 4 was greatly less than condition 3 ($t = -2.21, p = 0.04$) and condition 2 less than condition 1 ($-2.48, p = 0.02$). Percentage transition times in condition 3 was greatly less than condition 4 ($t = 2.39, p = 0.02$). Pupil diameter decreased from condition 1-3 ($t = -2.93, p = 0.01$) and $t = -3.29, p < 0.01$) and increased from condition 3-4 ($t = 2.59, p = 0.01$).

Table 11. The summary of significant results in pupil-related features. Values are presented as median \pm standard deviation. Bold values indicate significant results with a p-value less than 0.05. Values in task: 1 means monitoring task, 2 means check task, 3 means response task.

Feature	Task	C1	C2	C3	C4	p C2-C1	p C3-C2	p C4-C3
Duration [s]	3	22.62 \pm 4.56	20.61 \pm 4.73	20.67 \pm 4.06	19.03 \pm 2.74	0.02	0.94	0.04
Percentage Transition Times [%]	1	31.12 \pm 12.07	30.25 \pm 11.89	30.36 \pm 11.43	36.10 \pm 16.72	0.71	0.95	0.02
Pupil left avg	2	765.62 \pm 227.20	767.62 \pm 214.42	727.42 \pm 200.13	723.69 \pm 218.04	0.86	< 0.01	0.98
Pupil right avg	1	804.64 \pm 154.96	785.83 \pm 179.94	770.75 \pm 199.82	816.48 \pm 258.55	0.01	0.27	0.01
Pupil right avg	2	806.17 \pm 145.28	802.25 \pm 179.40	782.20 \pm 185.46	816.61 \pm 252.90	0.02	0.14	0.05
Pupil right avg	3	782.45 \pm 147.29	768.69 \pm 183.24	762.66 \pm 209.55	788.31 \pm 275.54	0.02	0.70	0.26

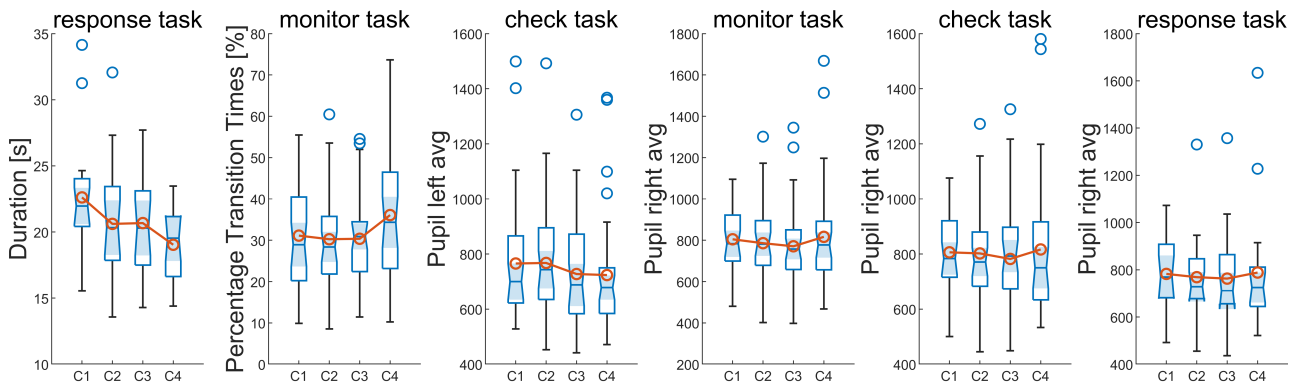


Figure 13. The boxplots display significant results in pupil-related features. Red lines represent average values.

Heat map. As shown in Figure 14, the heat map revealed attention distribution on each interest page. In condition 1 (row 2), heat distribution was wider to gather more information. In condition 2 (row 3), distribution was more precise and focused on AOIs. In condition 3 (row 4), areas near AOIs and confusing information got more fixation. In condition 4 (row 5), glances were messy on interest pages. Furthermore, within the procedure of experiment in every condition (column 1 and column 4, 2 and 5, 3 and 6), distribution was messier as the result of workload accumulation in the hot and humid environment.

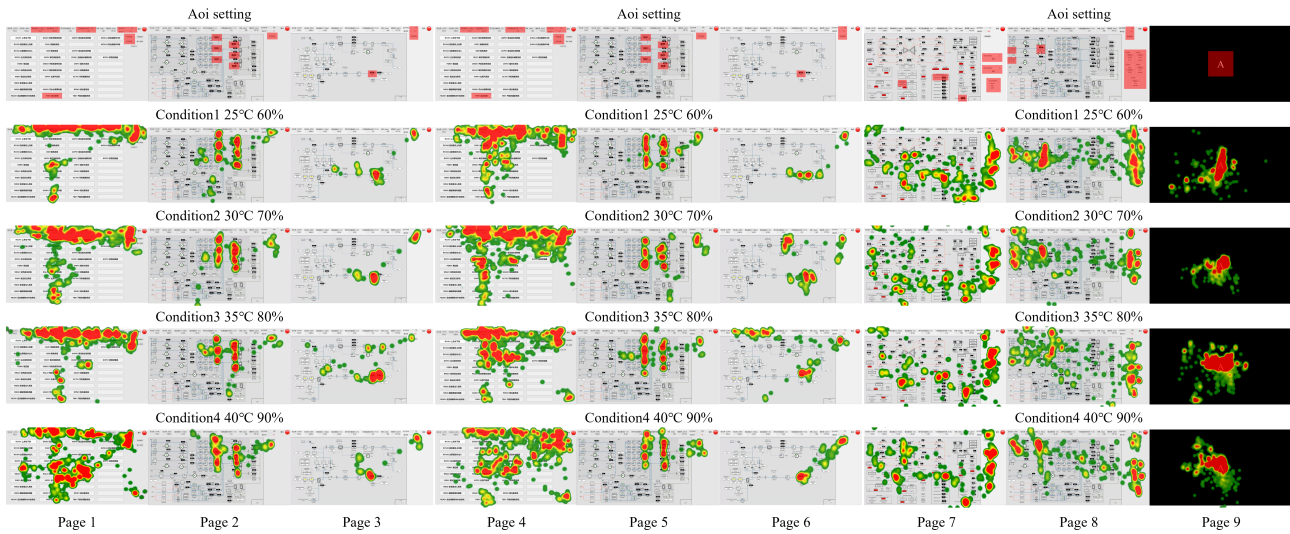


Figure 14. The heat map. Row 1: AOI settings in every interest page. Row 2-5: condition 1-4. Column 1-3: interest pages in the major task 1: fault detection task. Column 4-6: interest pages in the major task 2: fault detection task. Column 7-8: interest pages in the major task 3: operation task. Column 9: 2-back task.

4 DISCUSSION

4.1 *The effect of hot and humid environment on task performance and cognitive functions*

Among all conditions, no difference was observed in the task completion rate, SA level 1 perception score, and SA level 3 projection score. This suggests that high temperature and humidity had little impact on the completion rate. However, they did have a significant influence on the time and accuracy of the NPPs task.

In condition 1, longer fault detection time and fault confirmation time with higher temporal demand were observed. The result revealed that the performance would decline slightly at low temperature and humidity, which was also proved by Pilcher (Pilcher et al., 2002). He explored the threshold of the maximal adaptability model by meta-analysis and found that there was a negative influence on reasoning, learning, and memory tasks under 21.11°C WBGT (condition 1 was 21.26°C WBGT in our study). Our studies suggest that this is caused by nervous mode at the beginning of an emergency.

In condition 2, shorter fault detection time, fault confirmation time, and task completion time along with lower temporal demand as well as the lowest task load index and fewer missed numbers in the 2-back tasks were obtained. These results suggest that an environment in 26.88°C WBGT was suitable for operators with lower workload, calmer disposition, and better working memory, ultimately leading to better performance. The finding was supported by the inverse U-shaped model and the maximal adaptability model. Furthermore, Pilcher (Pilcher et al., 2002) found a small improvement in

reasoning, learning, and memory tasks when exposed to a hot environment of 26.67°C WBGT or above.

In condition 3, there were more errors (clicking on the wrong place or making incorrect decisions) in the operation task and a lower SA level 2 comprehension score which meant more mistakes and weaker comprehensive ability leading to poorer performance. The decrease was predicted by the maximal adaptability model and has been mentioned by several studies. Ramsey (Ramsey, 1995) found a significant performance decrement in perceptual-motor tasks (for example, alerting and operating equipment) between 30°C WBGT and 33°C WBGT (condition 3 was 31.92°C WBGT in our study). Pilcher (Pilcher et al., 2002) mentioned a great performance decline beyond 32.22°C WBGT.

In condition 4 (36.81°C WBGT), shorter task completion time, and shorter mean reaction time of all correct responses were presented which demonstrated faster response in simple reaction tasks because of stress response under extreme heat stress. Additionally, the most missed numbers in the 2 back task, the worst SAGAT total score, and the worst communication score with higher physical demand and higher effort were presented. The results indicated that extreme heat stress would lead to a rapid decline in complex tasks (i.e. teamwork) and cognitive functions (i.e. situation awareness, working memory) because of the fast accumulation of physical load and mental load, which was opposite to the improvement in the simple task. The similar phenomenon has been observed in numerous studies. Lovingood (Lovingood et al., 1967) found shorter reaction time, higher classification accuracy, and better calculation ability with worse arm stability under high temperature (52°C compared to 23.3°C). Hancock (Hancock and Vasmatazidis, 2003) reviewed that simple performance improved under a 10-minute short-term 43°C WBGT hot exposure. Tian (Tian et al., 2021) studied humidity influence and found that 70% relative humidity (RH) could lead to worse spatial perception, concentration, working memory, arousal level, and fatigue compared to 50% RH. Gaoua (Gaoua et al., 2011) investigated the heat exposure influence on cognitive functions and found that compared to 20°C, heat discomfort under 50°C would impair performance on complex cognitive tasks and working memory function. Although the participants in the high-temperature group responded faster, they spent more time finding the right solution (Gaoua et al., 2012).

4.2 Physiological-psychological mechanism of impairment on performance and cognitive functions in the hot and humid environment

4.2.1 Neural activity based on ECG and HRV

Performance decrement around 32°C WBGT (condition 3) and unsustainable state around 37°C WBGT (condition 4) could be explained by more tension, worse regulation ability, increasing stress, and mental load reflected by faster HR,

lower RMSSD, lower SDDSD, lower SDNN, lower PNN50, higher LF/HF and lower vagal.

Heart rate (HR), the number of heartbeats per minute, usually increases with heat stress (Abbasi et al., 2020) indicating increasing tension, stress, and mental load (Hwang et al., 2008; De Rivecourt et al., 2008). Heart rate variability (HRV), the relative change in the RR interval between two adjacent heartbeats, generally decreases as a result of stress (Shaffer et al., 2014; Hwang et al., 2008) and decreases with increasing task load (De Rivecourt et al., 2008). The indices describing heart rate variability, such as RMSSD, SDDSD, SDNN, and PNN50 (Chen et al., 2020), often indicate the adaptability of the nervous system to internal and external changes (Shaffer et al., 2014), and generally decrease with the increase of pressure and load (Hwang et al., 2008; Pakarinen et al., 2018).

The high-frequency component of the ECG signal (HF) is primarily associated with the activation of the parasympathetic nervous system (Delaney and Brodie, 2000), mainly represented by the vagal nerve. Activation of the vagal nerve, also known as the rest and digest system, is often accompanied by physiological activities such as miosis, heart rate slowing, and bronchoconstriction. The low-frequency component of the ECG signal (LF) mainly reflects the combined activation of the sympathetic and the parasympathetic nervous system (Martelli et al., 2014), along with physiological activities such as salivation. Therefore, LF/HF is commonly used as an index that reflects the balance between the activation of the sympathetic and parasympathetic nervous systems. It generally increases with pressure (Guasti et al., 2005) and mental load (Hwang et al., 2008). The higher LF/HF under heat stress was also reported in several studies (Lan et al., 2010; Abbasi et al., 2020).

Applying time-frequency analysis, a frequency band of approximately 1.5 Hz was identified. In the same condition, the PSD of the frequency band increased across different tasks associated with accumulating workload. However, there was a decrease in PSD during the final task, suggesting that additional cognitive resources could be collected with effort when participants knew that the procedure was near to end. Moreover, within the same task, the band frequency, high-frequency component, and overall PSD grew with temperature and humidity. This indicates an accumulating workload and chaotic heart activity.

4.2.2 Energy metabolism based on fNIRS

In the study, the detection task had more activated channels (betas significantly differ from 0) than the operation task and more channels were activated in the range of 27-32°C WBGT (condition 2 and 3). According to the neurovascular coupling mechanism, the neural activity of the brain increases during cognitive activities. As task difficulty (Causse et al.,

2017) or fatigue level (Pan et al., 2019) increases, there is a regular increment in the activation intensity in the PFC, which is caused by the increasing cognitive resources input and energy consumption of the cognitive functional brain areas.

The different performance trends between condition 2 and 3, despite the same PFC activation, could be explained by the neural efficiency hypothesis of intelligent individuals (Neubauer and Fink, 2009). The hypothesis claims that more intelligent individuals are able to achieve the same performance while investing fewer cognitive resources and experiencing lower brain activation. With learning and practice, operations might become more automatic and disassociated from PFC activation. Consequently, for more experienced and intelligent individuals, better task performance is associated with lower PFC activation, whereas the opposite holds true for less experienced and intelligent individuals. According to the hypothesis, the activation intensity can reveal the level of mental load (Ayaz et al., 2012), but has no significant correlation with task performance (Causse et al., 2017; Matsuda and Hiraki, 2006). During cognitive tasks in sleep-deprived states, activities in the prefrontal cortex were found to either increase due to compensatory mechanisms or decrease due to cognitive deficits (Pan et al., 2019).

Therefore, activation in condition 2 indicates an effective cognitive resource input and results in a good performance. In contrast, increased activation in condition 3 was explained by a compensatory mechanism due to fatigue, drowsiness, and slowed thinking. Reduced activation under the highest heat stress conditions (condition 4) indicates inhibition in the prefrontal cortex, an important cortex associated with decision-making, cognitive control, and working memory (Qian et al., 2020).

Applying resting-state functional connectivity analysis, higher synchronization in both time and frequency, which suggests higher cooperation between different brain regions, was observed in the hottest and most humid condition. FC strength is usually associated with fatigue, task complexity, and cognitive control. The global functional connectivity strength increases with the task difficulty and cognitive control (Cole et al., 2012), which was a potential explanation for the fastest response under the heaviest heat stress.

4.2.3 Visual search pattern based on Eye Tracking

In the AOI analysis, a greater saccade angle was obtained in condition 2, which meant more accurate search paths associated with a more efficient search strategy under suitable temperature and humidity.

In condition 3, we gained a greater number of fixations, longer total glance time, and mean glance duration. Fixation refers to the visual gaze remaining at a particular location, which generally lasts for 200-500 milliseconds. The fixation

rate is positively correlated with workload (Wu et al., 2020). The number of fixations can be used to judge whether individuals need to frequently observe and search on the interface to obtain enough information. Fixation time can be used to estimate the difficulty of extracting information on the page, which has a positive correlation (Wu et al., 2020).

Meanwhile, we noticed a lower percentage of transition times in condition 3 than in adjacent conditions. Saccades refer to the shifting of the eye between fixations, and generally the frequency of saccades decreases with increasing task difficulty, mental load, and cumulative fatigue (Wu et al., 2020; Nakayama et al., 2002).

In condition 4, we got more vertical eye activity which indicates worse concentration. Additionally, we observed a shorter mean fixation duration revealing a temporary improvement in cognitive efficiency.

The pupil diameter is mainly regulated by internal and external factors. The external factor is light conditions, where darker light leads to a larger pupil diameter. The internal factor is cognitive resources, i.e. mental effort and arousal. Larger pupil diameter is consistently associated with higher cognitive resource investment (Van Der Wel and Van Steenbergen, 2018), mental load, and task complexity (Batmaz and Ozturk, 2007). The average pupil diameter of the right eye in condition 4 was significantly larger than that in condition 3, indicating that the psychological load in condition 4 increased sharply in the extremely high-temperature and high-humidity environment, resulting in more mental effort to maintain the same performance. The second largest pupil appeared in condition 1, as participants were more nervous and excited with heavier cognitive load and arousal. In condition 2, where the temperature and humidity were suitable, a moderate arousal level and pupil diameter were observed. The smallest pupil was found in condition 3, which suggests that it was difficult to keep sufficient arousal in a sleepy state at high temperature and humidity.

The result of the heating map revealed that the visual search area in condition 1 was relatively wide, and operators needed to receive more information for adequate situation awareness and understanding, which corresponded to the search pattern under a nervous mode. In condition 2, the search pattern was more precise and operators browsed less in the areas outside the key information which ensured more efficient understanding and better task performance. In condition 3, the participants paid more attention to the confusing information and the areas outside the crucial information, which was consistent with the search pattern under a drowsy state. In condition 4, the fixation area was more chaotic because it was difficult to concentrate in the extremely high temperature and humidity environment.

Meanwhile, under the same condition, it was evident that the attention area outside the AOI in the major task 2 is considerably larger than that of the major task 1. This indicated a rapid increase in cognitive load and a decline in performance within a brief period of time (approximately 5 minutes).

4.3 The modified maximal adaptability model

In the range of common temperature and humid conditions, the maximal adaptability model (Hancock and Vasmatazidis, 2003) has been extensively acknowledged to describe the relationship between performance and environment. Up to now, only a few studies have investigated the performance in the extreme WBGT environment (Lovingood et al., 1967; Hancock and Vasmatazidis, 2003). However, the model has not been extended to the extreme WBGT environment. We carried out the experiment over 35°C WBGT (36.81 °C WBGT, condition 4) which was close to the human thermal limit within a safe workspace. A temporary simple improved performance was observed, which we attribute to increased cooperation among PFC. Under extreme heat stress, humans respond faster in simple reaction tasks due to stress response, however, load accumulation leads to a rapid decline in complex cognitive functions. The rapid accumulation of workload, both in physical load shown by the highest physical demand score in the NASA-TLX scale and the mental load shown by the biggest pupil from the eye tracking, limited further performance improvement in simple tasks. Additionally, another limitation was the impaired concentration supported by the evidence from the chaotic eye movements and intense ECG activities.

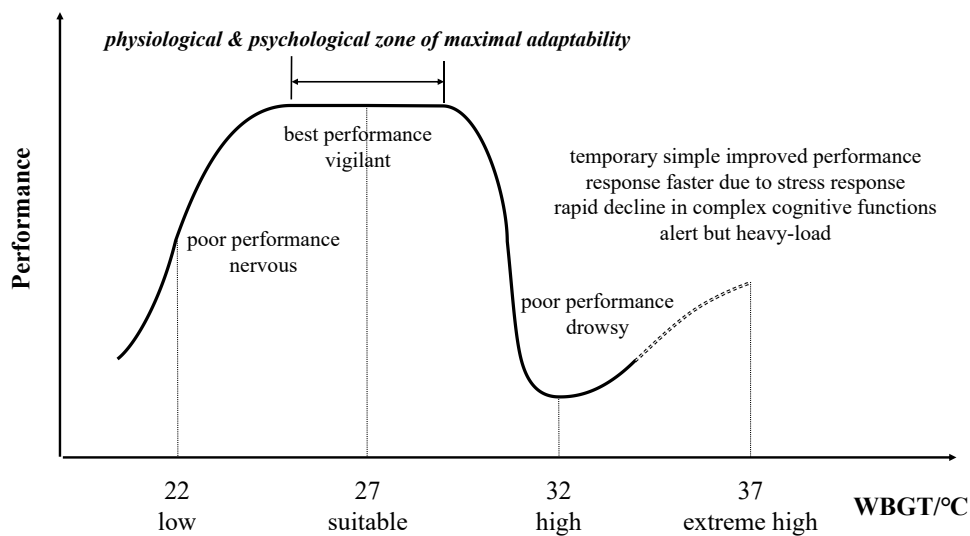


Figure 15. The modified maximal adaptability model extended to the extremely high temperature and humid environment with a temporary improvement in simple reaction tasks but a rapid decline in advanced cognitive functions.

5 CONCLUSION

From a neuroergonomics perspective, this study explored the performance in 21.26 °C, 26.88 °C, 31.92 °C, 36.81 °C WBGT and its underlying physiological-psychological mechanism based on ECG, fNIRS, and eye tracking. We verified and extended the maximal adaptability model to extremely high temperature and humid conditions over 35°C WBGT. Performance under 36.81°C WBGT could be described and explained by the maximal adaptability model with an extended inverse U shape. Unexpectedly, a temporary simple performance improvement was observed in the hottest and most humid environment. At low temperature and humidity (21.26 °C WBGT, condition 1), higher temporal demand in NASA-TLX and imprecise visual search patterns in the heat map showed that bad performance and slower response were caused by nervous mode. In a suitable environment at 26.88 °C WBGT (condition 2), enhanced performance with improved working memory and the lowest physical load was observed, which was driven by effective PFC activation and a more accurate search strategy (supported by heat map and greater saccade angle). With growing temperature and humidity, decreasing performance with more mistakes was related to worse understanding and drowsiness at 31.92°C WBGT (condition 3). The evidence from more activated PFC channels associated with compensatory mechanisms was provided by GLM. More fixation numbers and duration from eye tracking suggested worse information search and processing efficiency. The smallest pupil revealed the lowest arousal and the heat map showed more concentration on confusing information. In the last most extreme environment (36.81 °C WBGT, condition 4), there was a temporary simple improvement in simple reaction tasks that could be attributed to more brain connectivity, indicating more cooperation among PFC. The shorter fixation duration and the largest pupil demonstrated an improvement in information processing and arousal. As a result, participants respond faster in simple reaction tasks due to stress response. However, the simple improvement could not be sustained for a long time, and complex cognitive functions (i.e. situation awareness, communication, working memory) were impaired extremely, because of the difficulty in concentration with chaotic visual search heating map and increased vertical eye activity. Evidence from ECG also showed heavier load, poorer regulation ability, and increasing stress, as reflected by faster HR, lower HRV (RMSSD, SDSD, SDNN, PNN50), higher LF/HF, and lower vagal in the extreme environment.

This work provides a more detailed analysis of the process of performance and typical cognitive functions and executive functions under increasing heat stress. This can help to improve personnel management and emergency plans under hazards. In addition, the physiological-psychological mechanism underlying performance and typical functions were ex-

plored, which helped understand the interaction between operators' performance and workplace conditions under extreme heat strain, and supported that features extracted by specialized neuroscience methods could be potential biomarkers of cognitive performance under hot-humid exposures.

This work still has several limitations. Although we extend the maximal adaptability model to extreme heat conditions, four conditions are relatively insufficient to outline an accurate model. Moreover, our work supports a qualitative model which is inconvenient for monitoring the abnormal status of operators during production. In the future, we aim to develop a performance evaluation model based on psychological data and deep-learning networks to provide a real-time warning system for operators' abnormal states.

6 ACKNOWLEDGMENT

This study is supported by the State Key Laboratory of Nuclear Power Safety Technology and Equipment, China Nuclear Power Engineering Co., Ltd. (No.K-A2021.402), and the National Natural Science Foundation of China (No. 72374118, 72304165, 72204136).

REFERENCES

- , 2004. Human reliability data, human error and accident models—illustration through the three mile island accident analysis. *Reliability Engineering & System Safety* 83, 153–167.
- Abbasi, A.M., Motamedzade, M., Aliabadi, M., Golmohammadi, R., Tapak, L., 2020. Combined effects of noise and air temperature on human neurophysiological responses in a simulated indoor environment. *Applied Ergonomics* 88, 103189. URL: <https://www.sciencedirect.com/science/article/pii/S0003687018303703>, doi:<https://doi.org/10.1016/j.apergo.2020.103189>.
- Ayaz, H., Shewokis, P.A., Bunce, S., Izzetoglu, K., Willems, B., Onaral, B., 2012. Optical brain monitoring for operator training and mental workload assessment. *NeuroImage* 59, 36–47. URL: <https://www.sciencedirect.com/science/article/pii/S1053811911006410>, doi:<https://doi.org/10.1016/j.neuroimage.2011.06.023>. neuroergonomics: The human brain in action and at work.
- Batmaz, I., Ozturk, M., 2007. Using Pupil Diameter Changes for Measuring Mental Workload under Mental Processing.

- Journal of Applied Sciences 8, 68–76. URL: <https://www.scialert.net/abstract/?doi=jas.2008.68.76>, doi:10.3923/jas.2008.68.76.
- Causse, M., Chua, Z., Peysakhovich, V., Del Campo, N., Matton, N., 2017. Mental workload and neural efficiency quantified in the prefrontal cortex using fNIRS. *Scientific Reports* 7, 5222. URL: <https://www.nature.com/articles/s41598-017-05378-x>, doi:10.1038/s41598-017-05378-x.
- Chang, C.H., Bernard, T.E., Logan, J., 2017. Effects of heat stress on risk perceptions and risk taking. *Applied Ergonomics* 62, 150–157. URL: <https://www.sciencedirect.com/science/article/pii/S0003687017300546>, doi:<https://doi.org/10.1016/j.apergo.2017.02.018>.
- Chen, Y., Tao, M., Liu, W., 2020. High temperature impairs cognitive performance during a moderate intensity activity. *Building and Environment* 186, 107372. URL: <https://www.sciencedirect.com/science/article/pii/S0360132320307411>, doi:<https://doi.org/10.1016/j.buildenv.2020.107372>.
- Chen, Y., Wang, Z., Tian, X., Liu, W., 2023. Evaluation of cognitive performance in high temperature with heart rate: A pilot study. *Building and Environment* 228, 109801. URL: <https://www.sciencedirect.com/science/article/pii/S0360132322010319>, doi:<https://doi.org/10.1016/j.buildenv.2022.109801>.
- Cole, M.W., Yarkoni, T., Repovš, G., Anticevic, A., Braver, T.S., 2012. Global connectivity of prefrontal cortex predicts cognitive control and intelligence. *Journal of Neuroscience* 32, 8988–8999.
- De Rivecourt, M., Kuperus, M.N., Post, W.J., Mulder, L.J., 2008. Cardiovascular and eye activity measures as indices for momentary changes in mental effort during simulated flight. *Ergonomics* 51, 1295–1319. URL: <https://www.tandfonline.com/doi/full/10.1080/00140130802120267>, doi:10.1080/00140130802120267.
- Delaney, J.P.A., Brodie, D.A., 2000. Effects of Short-Term Psychological Stress on the Time and Frequency Domains of Heart-Rate Variability. *Perceptual and Motor Skills* 91, 515–524. URL: <http://journals.sagepub.com/doi/10.2466/pms.2000.91.2.515>, doi:10.2466/pms.2000.91.2.515.
- Endsley, M., 1988. Situation awareness global assessment technique (sagat), in: *Proceedings of the IEEE 1988 National Aerospace and Electronics Conference*, pp. 789–795 vol.3. doi:10.1109/NAECON.1988.195097.
- Gaoua, N., Grantham, J., Racinais, S., El Massioui, F., 2012. Sensory displeasure reduces complex cognitive performance in the heat. *Journal of Environmental Psychology* 32, 158–163. URL: <https://>

www.sciencedirect.com/science/article/pii/S0272494412000035, doi:<https://doi.org/10.1016/j.jenvp.2012.01.002>.

Gaoua, N., Racinais, S., Grantham, J., El Massioui, F., 2011. Alterations in cognitive performance during passive hyperthermia are task dependent. *International Journal of Hyperthermia* 27, 1–9. URL: <http://www.tandfonline.com/doi/full/10.3109/02656736.2010.516305>, doi:10.3109/02656736.2010.516305.

Guasti, L., Simoni, C., Mainardi, L., Crespi, C., Cimpanelli, M., Klersy, C., Gaudio, G., Grandi, A.M., Cerutti, S., Venco, A., 2005. Global link between heart rate and blood pressure oscillations at rest and during mental arousal in normotensive and hypertensive subjects. *Autonomic Neuroscience* 120, 80–87. URL: <https://www.sciencedirect.com/science/article/pii/S1566070205000342>, doi:<https://doi.org/10.1016/j.autneu.2005.02.008>.

Hancock, P.A., 1989. A Dynamic Model of Stress and Sustained Attention. *Human Factors: The Journal of the Human Factors and Ergonomics Society* 31, 519–537. URL: <http://journals.sagepub.com/doi/10.1177/001872088903100503>, doi:10.1177/001872088903100503.

Hancock, P.A., Vasmatazidis, I., 2003. Effects of heat stress on cognitive performance: the current state of knowledge. *International Journal of Hyperthermia* 19, 355–372. URL: <https://www.tandfonline.com/doi/full/10.1080/0265673021000054630>, doi:10.1080/0265673021000054630.

Hou, X., Zhang, Z., Zhao, C., Duan, L., Gong, Y., Li, Z., Zhu, C., 2021. NIRS-KIT: a MATLAB toolbox for both resting-state and task fNIRS data analysis. *Neurophotonics* 8. URL: <https://www.spiedigitallibrary.org/journals/neurophotonics/volume-8/issue-01/010802/NIRS-KIT--a-MATLAB-toolbox-for-both-resting-state/10.1117/1.NPh.8.1.010802.full>, doi:10.1117/1.NPh.8.1.010802.

Hwang, S.L., Yau, Y.J., Lin, Y.T., Chen, J.H., Huang, T.H., Yenn, T.C., Hsu, C.C., 2008. Predicting work performance in nuclear power plants. *Safety Science* 46, 1115–1124. URL: <https://www.sciencedirect.com/science/article/pii/S0925753507000872>, doi:<https://doi.org/10.1016/j.ssci.2007.06.005>.

Jiang, Q., Yang, X., Liu, K., Li, B., Li, L., Li, M., Qian, S., Zhao, L., Zhou, Z., Sun, G., 2013. Hyperthermia impaired human visual short-term memory: An fMRI study. *International Journal of Hyperthermia* 29, 219–

224. URL: <http://www.tandfonline.com/doi/full/10.3109/02656736.2013.786141>, doi:10.3109/02656736.2013.786141.

Kim, H., Hong, T., Kim, J., Yeom, S., 2020. A psychophysiological effect of indoor thermal condition on college students' learning performance through eeg measurement. *Building and Environment* 184, 107223. URL: <https://www.sciencedirect.com/science/article/pii/S0360132320305941>, doi:<https://doi.org/10.1016/j.buildenv.2020.107223>.

Lan, L., Lian, Z., Pan, L., 2010. The effects of air temperature on office workers' well-being, workload and productivity-evaluated with subjective ratings. *Applied Ergonomics* 42, 29–36. URL: <https://www.sciencedirect.com/science/article/pii/S000368701000058X>, doi:<https://doi.org/10.1016/j.apergo.2010.04.003>.

Liu, C., Zhang, Y., Sun, L., Gao, W., Jing, X., Ye, W., 2021. Influence of indoor air temperature and relative humidity on learning performance of undergraduates. *Case Studies in Thermal Engineering* 28, 101458. URL: <https://www.sciencedirect.com/science/article/pii/S2214157X21006213>, doi:<https://doi.org/10.1016/j.csite.2021.101458>.

Liu, K., Sun, G., Li, B., Jiang, Q., Yang, X., Li, M., Li, L., Qian, S., Zhao, L., Zhou, Z., von Deneen, K.M., Liu, Y., 2013. The impact of passive hyperthermia on human attention networks: An fmri study. *Behavioural Brain Research* 243, 220–230. URL: <https://www.sciencedirect.com/science/article/pii/S0166432813000235>, doi:<https://doi.org/10.1016/j.bbr.2013.01.013>.

Liu, W., Tian, X., Tao, M., 2022. A model to quantify the relation between cognitive performance and thermal responses in high temperature at a moderate activity level. *Building and Environment* 207, 108431. URL: <https://www.sciencedirect.com/science/article/pii/S0360132321008283>, doi:<https://doi.org/10.1016/j.buildenv.2021.108431>.

Lovingood, B.W., Blyth, C.S., Peacock, W.H., Lindsay, R.B., 1967. Effects of d-Amphetamine Sulfate, Caffeine, and High Temperature on Human Performance. *Research Quarterly. American Association for Health, Physical Education and Recreation* 38, 64–71. URL: <https://www.tandfonline.com/doi/full/10.1080/10671188.1967.10614804>, doi:10.1080/10671188.1967.10614804.

- Malmo, R.B., Malmo, H.P., 2000. On electromyographic (emg) gradients and movement-related brain activity: significance for motor control, cognitive functions, and certain psychopathologies. *International Journal of Psychophysiology* 38, 143–207. URL: <https://www.sciencedirect.com/science/article/pii/S0167876000001136>, doi:[https://doi.org/10.1016/S0167-8760\(00\)00113-6](https://doi.org/10.1016/S0167-8760(00)00113-6).
- Martelli, D., Silvani, A., McAllen, R.M., May, C.N., Ramchandra, R., 2014. The low frequency power of heart rate variability is neither a measure of cardiac sympathetic tone nor of baroreflex sensitivity. *American Journal of Physiology-Heart and Circulatory Physiology* 307, H1005–H1012. URL: <https://www.physiology.org/doi/10.1152/ajpheart.00361.2014>, doi:[10.1152/ajpheart.00361.2014](https://doi.org/10.1152/ajpheart.00361.2014).
- Matsuda, G., Hiraki, K., 2006. Sustained decrease in oxygenated hemoglobin during video games in the dorsal prefrontal cortex: A nirs study of children. *NeuroImage* 29, 706–711. URL: <https://www.sciencedirect.com/science/article/pii/S1053811905006233>, doi:<https://doi.org/10.1016/j.neuroimage.2005.08.019>.
- Nakata, H., Kakigi, R., Shibasaki, M., 2021. Effects of passive heat stress and recovery on human cognitive function: An ERP study. *PLOS ONE* 16, e0254769. URL: <https://dx.plos.org/10.1371/journal.pone.0254769>, doi:[10.1371/journal.pone.0254769](https://doi.org/10.1371/journal.pone.0254769).
- Nakayama, M., Takahashi, K., Shimizu, Y., 2002. The act of task difficulty and eye-movement frequency for the 'Oculomotor indices', in: *Proceedings of the symposium on Eye tracking research & applications - ETRA '02*, ACM Press, New Orleans, Louisiana. p. 37. URL: <http://portal.acm.org/citation.cfm?doid=507072.507080>, doi:[10.1145/507072.507080](https://doi.org/10.1145/507072.507080).
- Neubauer, A.C., Fink, A., 2009. Intelligence and neural efficiency. *Neuroscience & Biobehavioral Reviews* 33, 1004–1023. URL: <https://www.sciencedirect.com/science/article/pii/S0149763409000591>, doi:<https://doi.org/10.1016/j.neubiorev.2009.04.001>.
- O'Hara, J., Higgins, J., Brown, W., Fink, R., Persensky, J., Lewis, P., Kramer, J., Szabo, A., Boggi, M., 2008. Human factors considerations with respect to emerging technology in nuclear power plants. US Nuclear Regulatory Commission, Washington, DC, USA .
- Pakarinen, S., Korpela, J., Torniainen, J., Laarni, J., Karvonen, H., 2018. Cardiac measures of nuclear power plant

- operator stress during simulated incident and accident scenarios. *Psychophysiology* 55, e13071. URL: <https://onlinelibrary.wiley.com/doi/10.1111/psyp.13071>, doi:10.1111/psyp.13071.
- Pan, Y., Borragnán, G., Peigneux, P., 2019. Applications of Functional Near-Infrared Spectroscopy in Fatigue, Sleep Deprivation, and Social Cognition. *Brain Topography* 32, 998–1012. URL: <http://link.springer.com/10.1007/s10548-019-00740-w>, doi:10.1007/s10548-019-00740-w.
- Pilcher, J.J., Nadler, E., Busch, C., 2002. Effects of hot and cold temperature exposure on performance: a meta-analytic review. *Ergonomics* 45, 682–698. URL: <https://www.tandfonline.com/doi/full/10.1080/00140130210158419>, doi:10.1080/00140130210158419.
- Provins, K.A., 1966. Environmental heat, body temperature and behaviour: An hypothesis. *Australian Journal of Psychology* 18, 118–129. URL: <https://www.tandfonline.com/doi/full/10.1080/00049536608255722>, doi:10.1080/00049536608255722.
- Qian, S., Zhang, J., Yan, S., Shi, Z., Wang, Z., Zhou, Y., 2020. Disrupted Anti-correlation Between the Default and Dorsal Attention Networks During Hyperthermia Exposure: An fMRI Study. *Frontiers in Human Neuroscience* 14, 564272. URL: <https://www.frontiersin.org/articles/10.3389/fnhum.2020.564272/full>, doi:10.3389/fnhum.2020.564272.
- Ramsey, J.D., 1995. Task performance in heat: a review. *Ergonomics* 38, 154–165. URL: <http://www.tandfonline.com/doi/abs/10.1080/00140139508925092>, doi:10.1080/00140139508925092.
- Shaffer, F., McCraty, R., Zerr, C.L., 2014. A healthy heart is not a metronome: an integrative review of the heart’s anatomy and heart rate variability. *Frontiers in Psychology* 5. URL: <http://journal.frontiersin.org/article/10.3389/fpsyg.2014.01040/abstract>, doi:10.3389/fpsyg.2014.01040.
- for Standardization, I.O., 2017. *Ergonomics of the thermal environment — Assessment of heat stress using the WBGT (wet bulb globe temperature) index*. ISO 7243:2017 ed., International Organization for Standardization, Vernier, Geneva, Switzerland. URL: <https://www.iso.org/standard/63098.html>.
- Tan, X.R., Stephenson, M.C., Alhadad, S.B., Loh, K.W., Soong, T.W., Lee, J.K., Low, I.C., 2023. Elevated brain temperature under severe heat exposure impairs cortical motor activity and executive function. *Jour-*

nal of Sport and Health Science URL: <https://www.sciencedirect.com/science/article/pii/S2095254623000789>, doi:<https://doi.org/10.1016/j.jshs.2023.09.001>.

Tian, X., Fang, Z., Liu, W., 2021. Decreased humidity improves cognitive performance at extreme high indoor temperature. *Indoor Air* 31, 608–627. URL: <https://onlinelibrary.wiley.com/doi/10.1111/ina.12755>, doi:[10.1111/ina.12755](https://doi.org/10.1111/ina.12755).

Tran, C.C., Yan, S., Habiyaremye, J.L., Wei, Y., 2017. Predicting driver's work performance in driving simulator based on physiological indices, in: *Intelligent Human Computer Interaction: 9th International Conference, IHCI 2017, Evry, France, December 11-13, 2017, Proceedings 9*, Springer International Publishing. pp. 150–162.

Van Der Wel, P., Van Steenbergen, H., 2018. Pupil dilation as an index of effort in cognitive control tasks: A review. *Psychonomic Bulletin & Review* 25, 2005–2015. URL: <http://link.springer.com/10.3758/s13423-018-1432-y>, doi:[10.3758/s13423-018-1432-y](https://doi.org/10.3758/s13423-018-1432-y).

Visnovcova, Z., Mestanik, M., Gala, M., Mestanikova, A., Tonhajzerova, I., 2016. The complexity of electrodermal activity is altered in mental cognitive stressors. *Computers in Biology and Medicine* 79, 123–129. URL: <https://www.sciencedirect.com/science/article/pii/S0010482516302724>, doi:<https://doi.org/10.1016/j.combiomed.2016.10.014>.

Whaley, A.M., 2016. Cognitive basis for human reliability analysis. US Nuclear Regulatory Commission, Office of Nuclear Regulatory Research.

Wu, Y., Liu, Z., Jia, M., Tran, C.C., Yan, S., 2020. Using Artificial Neural Networks for Predicting Mental Workload in Nuclear Power Plants Based on Eye Tracking. *Nuclear Technology* 206, 94–106. URL: <https://www.tandfonline.com/doi/full/10.1080/00295450.2019.1620055>, doi:[10.1080/00295450.2019.1620055](https://doi.org/10.1080/00295450.2019.1620055).

Xu, X., Lu, Y., Vogel-Heuser, B., Wang, L., 2021. Industry 4.0 and industry 5.0—inception, conception and perception. *Journal of Manufacturing Systems* 61, 530–535. URL: <https://www.sciencedirect.com/science/article/pii/S0278612521002119>, doi:<https://doi.org/10.1016/j.jmsy.2021.10.006>.

Yeoman, K., Weakley, A., DuBose, W., Honn, K., McMurry, T., Eiter, B., Baker, B., Poplin, G., 2022. Effects of heat strain on cognitive function among a sample of miners. *Applied Ergonomics* 102, 103743. URL:

<https://www.sciencedirect.com/science/article/pii/S0003687022000667>, doi:<https://doi.org/10.1016/j.apergo.2022.103743>.

Zhu, H., Hu, M., Hu, S., Wang, H., Guan, J., 2023a. Effects of hot-humid exposure on human cognitive performance under sustained multi-tasks. *Energy and Buildings* 279, 112704. URL: <https://www.sciencedirect.com/science/article/pii/S0378778822008751>, doi:<https://doi.org/10.1016/j.enbuild.2022.112704>.

Zhu, H., Wang, Y., Hu, S., Ma, L., Su, H., Wang, J., 2023b. Cognitive performances under hot-humid exposure: An evaluation with heart rate variability. *Building and Environment* 238, 110325. URL: <https://www.sciencedirect.com/science/article/pii/S0360132323003529>, doi:<https://doi.org/10.1016/j.buildenv.2023.110325>.